# Memory effects in the autophagic response of S. cerevisiae

Eirik-Andreas Vestersjø

Supervisors: Nathalia Chica & Jorrit M. Enserink


Thesis submitted for the degree of
Master's in molecular biology and biochemistry
60 credits

Department of Bioscience
Faculty of Mathematics and natural sciences

UNIVERSITETET OF OSLO

Fall 2022

# Memory effects in the autophagic response of S. cerevisiae

Eirik-Andreas Verstersjø

Supervisors: Nathalia Chica & Jorrit M. Enserink

Supervisors: Nathalia Chica & Jorrit M. Enserink

Title

http://www.duo.uio.no/

Print: Reprosentralen, Universitetet i Oslo

# Acknowledgements

First and foremost, I would like to thank my co-supervisor Nathalia Chica. She has been patient and supportive even in situations where I'm not sure I deserved it. The depth of her knowledge and experience in the field has been a resource I could not have done without, and I would not have gotten as far as I have if it were not for her guidance. I truly respect and appreciate your dedication to your work and to your students, again thank you.

I also need to thank my main supervisor Professor and Group leader Jorrit M. Enserink for allowing me to work on this project in his group. It has been a delight and I truly appreciate your dedication both to the work we have done and the extraordinarily friendly and supportive work environment you have fostered. I have had difficult times in this project and your support has meant the world to me.

The rest of the Enserink lab also deserve thanks for all the help and guidance I have received as well as the happy social times we have had together. I could not have asked for better people to work with. A special thanks goes out to Aram N. Andersen for all the significant help I have received in data analysis and bioinformatics. I leave these two years with a much greater understanding then when I started, and you deserve a lot of credit for that. Linda Sønsterud has been one of the most supportive and nice people I have ever worked with, and I thank you for all the times you have shown me how to do things without becoming impatient when it takes me a second to understand.

I would also like to thank my friends for all their support. I could not have done this without knowing that whatever happened you would have my back. Benjamin and Selma, I could not ask for better roommates, I will always love you guys. Alberto, you have been like a brother to me through this process and there is no-one who could have understood me better during our projects. To all those friends that I have had less opportunity to see, Michelle, Delali, Nina, Gry and any others I might be forgetting, thank you for being so patient. My mother might truly be the greatest parent in the world, and I am so grateful for her support. They won't ever read it, but I would also like to thank Skygge and Darwin for being the loveliest little cat and dog I could have hoped for.

Oslo, December 2022
Eirik-Andreas Vestersjø

# Abbreviations

| | |
|---|---|
| ATG | Autophagy-related gene |
| ATP | Adenosine triphosphate |
| cAMP | Cyclic AMP |
| GAP | GTPase-activating protein |
| GDP | Guanosine diphosphate |
| GEF | Guanosine exchange factor |
| GFP | Green fluorescent protein |
| GO | Gene ontology |
| GTP | Guanosine triphosphate |
| H3K4 | Histone H3 Lysine 4 |
| LeuRS | Leucyl-tRNA synthetase |
| MRS | Memory recruitment sequence |
| NPC | Nuclear Pore Complex |
| NPP | Nuclear Pore Protein |
| PAS | Pre-autophagosomal structure/Phagophore assembly site |
| PI(3)P | Phosphatidylinositol 3-phosphate |
| PKA | Protein Kinase A |
| PtdIns3K | Phosphatidylinositol-3 kinase complex I |
| PtdIns4P | Phosphatidylinositol-4-phosphate |
| RAPTOR | Regulatory associated protein of mTOR |
| RNAPII | RNA polymerase II |
| SEACAT | Seh1-associated complex activating TOR |
| SEACIT | Seh1-associated complex inhibiting TOR |
| TOR | Target of rapamycin |
| TORC1 | Target of rapamycin complex 1 |
| TORC2 | Target of rapamycin complex 2 |
| WT | Wild Type |

# Abstract

Autophagy is the catabolic breakdown of old or dysfunctional cellular components like organelles, proteins, or other structures into new macromolecules that the cell can use to build components that are more suitable for the current needs of the cell. The process of autophagy is primarily controlled by the TORC1 complex and is initiated when TORC1 is deactivated because of a lack of nitrogen sources in the cell. If a cell goes through nitrogen starvation it is essential that its response is finely tuned in order to maximize the survival chances of the cell. One way yeast responds to a changing of nutrient availability is through the retention of previous conditions through cell memory. This retention of information has been found in response to the cell being forced to feed on galactose, a carbon source inferior to glucose, and inositol. Several generations after the initial stimulus *S. cerevisiae* re-activates its galactose machinery faster if it has cell memories of galactose. Whether nitrogen starvation induces the same memory response as galactose has never been examined.

This thesis investigated the potential for a memory effect in the process of autophagy by growing cells through cycles of starvation and replenishment. Using those results we conducted a large-scale screen using *S. cerevisiae* as a model organism to find proteins regulating this memory effect. Alongside this a set of biological assays were conducted to examine the biological underpinnings of the memory process.

Overall, the results indicated clearly that there is a memory effect present in yeast cells that becomes active between 4 and 5 hours into the initial stimulus. The screening also showed that some of the established machinery in other memory effects are needed for the memory effect in autophagy. Furthermore, we found that the most likely mechanism of this memory effect is a more rapid transcription of autophagy-related genes upon re-introduction to starvation conditions. Giving some proof to the presence of a memory effect in the autophagic response will hopefully lead to more research being done to elucidate the underlying mechanisms.

# Content

# List of tables

# List of figures

# Chapter 1

# Introduction

## 1.1 Autophagy: A historical perspective

Autophagy is fundamentally a way for cells to digest its components to gain new metabolites for the cell. By creating a large double-membraned structure that engulfs cellular components and transports them to the lysosome in mammals, or vacuole in yeast, the cell can maintain a steady access to metabolites to make new cellular components[1]. This evolutionarily conserved process is constantly ongoing at low levels in the cell to have turnover of aging, failing, or damaged proteins, organelles, or other cellular components. When the cell runs low on nutrients, the autophagic activity in cell rises to compensate. The term autophagy was first coined by Christian de Duve in 1963 when he discovered the lysosome in research using rat livers [2]. He gave the process the name autophagy, which is Greek for self-devouring. Autophagosomes, the double-membraned structures used to transport components to the vacuole or lysosome, were identified using electron microscopy through several experiments in the 1960s. Early in the 1980s studies by Pfiefer showed that autophagy was linked to circadian rhythms showing that fasting between meals induced autophagy and thus that autophagy is linked to nutrient levels[3]. Around the same time Mortimore and his group proved that protein degradation was increased when access to amino acids was limited, thus linking autophagy to nitrogen metabolism[4]. Work in the field of autophagy was slow, most of the work was done by electron microscopy which was difficult due to the heterogenous nature of autophagosomes and autophagolysosomes. The next major leap forwards was the discovery of the core autophagy genes by Yoshinori Ohsumi in the 1990s[5]. By working with *S. cerevisiae* as a model organism Ohsumi was able to establish Apg1Δ, now known as Atg1, as an autophagy-defective mutant. He did this by using a vacuolar protease inhibitor, which leads to the accumulation of autophagic bodies in the vacuole of WT cells during nitrogen starvation, and screening across mutants to find those that didn’t accumulate

autophagic bodies. Following the discovery that *apg1* mutants die under prolonged nitrogen starvation a screen was made that used that low viability as one of the main criteria. The screen was effective and identified most of the proteins involved in what is commonly known as the autophagy core machinery. This drove interest in the field to expand greatly and proved that *S. cerevisiae* is a powerful model organism to expand the understanding of the process. The number of ATG genes (AuTophaGy-related genes) currently characterized stands at 42 [6] and the understanding of pathways of degradation in autophagy has greatly expanded. For his work in autophagy, Ohsumi was in 2016 awarded the Nobel Prize in Physiology or Medicine by the Nobel assembly at Karolinska Institute.

Autophagy is both a basal process, active at all times, and a response to various conditions. Heat stress, nutrient starvation, and oxidative stress are all stressors that can cause the cell to enter autophagy. Given its fundamental role in the maintenance of the nutrient levels of cells, it should come to no surprise that a functional autophagy response is linked to the health of both individual cells and the whole organism. As the field of autophagy expands, the role of autophagy in medicine and health has expanded as well. Dysregulation of autophagy has been shown in neurodegenerative diseases like ALS and Alzheimer's[7], metabolic diseases like obesity[8] and diabetes mellitus[9], and cancer[10]. As work in these fields progresses, the role of autophagy will only become clearer.

## 1.2 Three general processes of Autophagy

Autophagy in cells take several forms to execute two related but distinct tasks, the degradation of old or damaged cellular components and the production of new metabolites from recycled cellular components. The degradation of cellular components keeps cells healthy by preventing the accumulation of damaged or ineffective proteins, organelles, or structures which can significantly affect the health of both the cell and the organism at large. Together the two sides of autophagy keep cellular components from becoming dysfunctional while allowing the dynamic relocation and application of resources depending on the needs of the cell. Thereby letting the cell adapt to changing circumstances and protecting it from potentially harmful effects of malfunctioning components. While there are many forms of autophagy it can generally divided into three categories, namely microautophagy, chaperone-mediated autophagy, and macroautophagy as shown in figure 1.1.

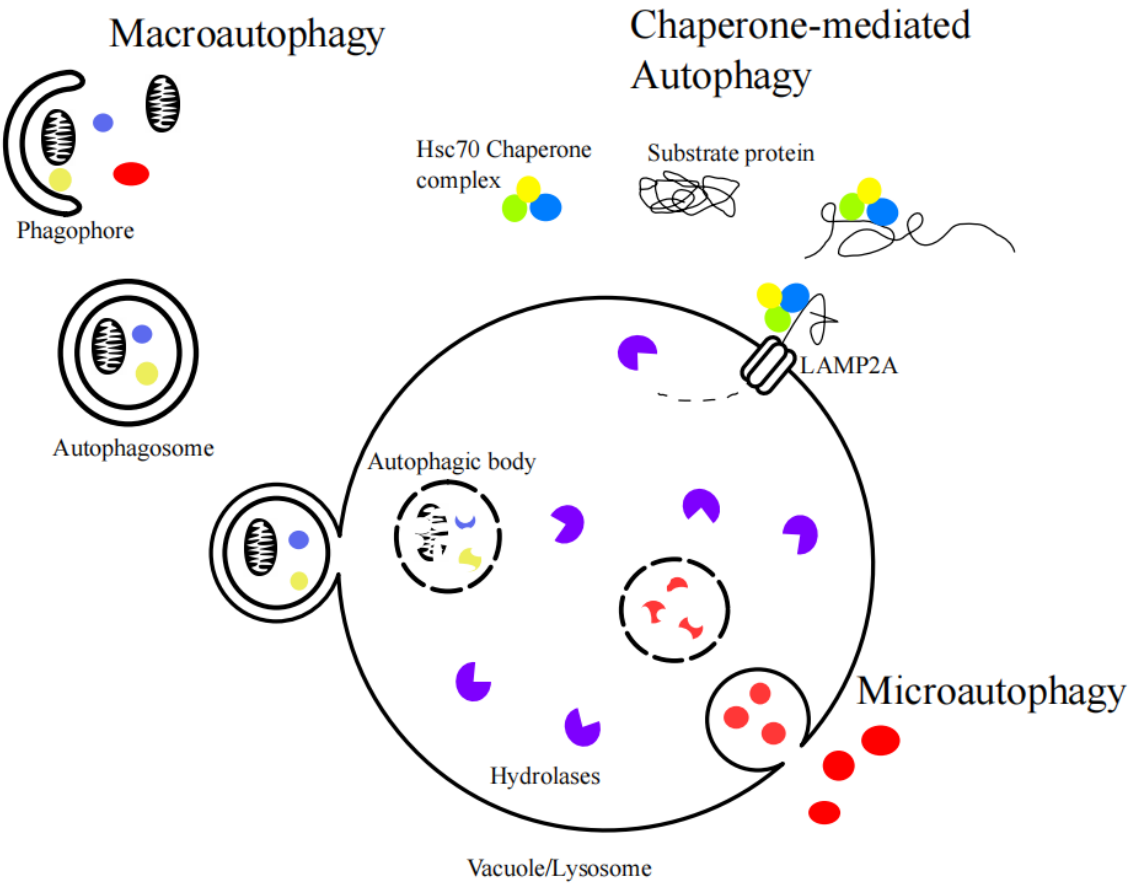


**Figure 1.1: The three main forms of autophagy.** A visualization of the different forms of autophagy. Macroautophagy involves the elongation of a phagophore around cytosolic components, either specifically or randomly at the phagophore assembly site. Once closed the phagophore has become an autophagosome which will fuse with the vacuolar/lysosomal membrane and the content will become an autophagic body in the vacuolar/lysosomal lumen before being broken down. Chaperone mediate autophagy begins with the recognition of the KFERQ motif by the chaperone proteins, which in turn bind the protein to lysosome-associated membrane protein type A which transports the protein into the lysosomal lumen. Microautophagy happens by the invagination of the membrane around the components, either specifically or randomly. The degradation products are transported out by vacuolar or lysosomal transporters.

Microautophagy occurs by the invagination of the vacuolar or lysosomal membrane around the target[11]. This form of autophagy can be both specific and non-specific. The non-specific form happens in virtually all eukaryotic cell types whereas the specific pathways are more limited in extent, micropexophagy, micromitophagy, and piecemeal microautophagy of the nucleus have all been observed in yeast cells. The experiments elucidating microautophagy have largely been conducted using yeast cells and so the process is not well understood in mammals though the process has been found to occur on late endosomes[12]. Chaperone-mediated autophagy is highly specific targeting of proteins for degradation in the lysosome. This mechanism has been described in mammals and other higher eukaryotes but does not appear in yeast. Chaperone-mediated autophagy requires substrate proteins that can be

unfolded and have a specific KFERQ motif that can be recognized and bound by HSC70 chaperone protein complexes. The KFERQ motif is found in approximately 40% of the proteins in the human proteome. The chaperone complex then binds to LAMP2A in the lysosomal membrane which leads to the translocation of the substrate protein into the lumen where it is degraded[13].

### 1.2.1 Macroautophagy in the cell

Macroautophagy is the most widely researched form of autophagy and the most researched. It is marked by the inactivation of the TORC1 complex leading to the formation of a double membraned structure called a phagophore[14]. This structure encapsulates cellular components at a cellular location known as the phagophore assembly site (PAS) in yeast or omegasome in mammals. Once the phagophore has fully engulfed the components and become a closed vesicle it is transported to the vacuole or lysosome where it fuses with the membrane so that its cargo and inner membrane is transferred into the lumen as an autophagic body and broken down. This form of autophagy can be non-specific, breaking down random cellular components caught in the phagophore to metabolites, it can however also be specific when organelles or other structures are marked for degradation. Macroautophagy is one of the main pathways by which organelles can be broken down and so most organelles have their own type of specific selective autophagic process, examples include mitophagy (mitochondria), pexophagy (peroxisomes), and lysophagy (lysosomes). Macroautophagy can also be used to break down foreign pathogens using xenophagy. The focus of this paper is non-selective macroautophagy which will from this point on be referred to as autophagy.

## 1.3 TORC1: Major negative regulator of autophagy

There is a constitutive basal level of autophagy present in all cells, but the levels change based on the nutritional state of the cells, especially the availability of nitrogen sources. This allows the autophagy response to be a dynamic process in changing environments. To sense and interpret the nutritional state, the cell uses complexes containing Target of Rapamycin (Tor) phosphatidylinositol kinases. These proteins are named so because they are inactivated by the drug rapamycin which binds to the proline rotamase FKBP12 and this complex then binds to

the FKBP12-rapamycin binding (FRB) domain in Tor proteins[15]. Unlike most other organisms, *S. cerevisiae* has two Tor kinases, Tor1 and Tor2, they are similar but not identical and form the core of two complexes related to growth in the cell, TORC1 and TORC2. Of these only TORC1 is sensitive to the nutrient status of the cell, whereas TORC2 is involved in the remodeling of the cytoskeleton and the biosynthesis of ceramides[16]. Notably, TORC2 is not affected by rapamycin because its FRB domain is inaccessible to rapamycin-FKBP12[15]. The inactivation of TORC1 induces autophagy in the cell and can be induced by a lack of access to nitrogen sources, specifically amino acids. Inactivation can also be artificially induced by treatment with rapamycin, a practice common in the study of autophagy. Importantly, the function of TORC1 as a nutrient sensor means it has wide-ranging functions in the cell outside of autophagy, including protein translation, ribosome biogenesis, and the suppression of stress responses[17]. Both TORC1 and TORC2 are well conserved complexes that can be found in almost all higher eukaryotes[18], the only exception being intracellular parasites.

## 1.3.1 The TORC1 and mTORC1 complexes

The TORC1 complex consists of the subunits Tor1 or Tor2, Kog1, Lst8, and Tco89, with only Tco89 being non-essential to the function of the complex. The function of Kog1 is to bind TORC1 to its activator on the vacuolar membrane[19]. Tco89 does appear to be important for the recovery from inactivation[20]. The mammalian equivalent to TORC1 is mTORC1 which serves many of the same functions including the induction of autophagy in response to a lack of nitrogen sources. Several of the subunits of TORC1 have mammalian homologues, the mTOR, mLST8, and RAPTOR (Regulatory Associated Protein of TOR) is a Kog1 homologue. mLST8 binds to the kinase domain of TOR and is necessary for the catalytic activity of the protein[21]. Which might be an indicator of its function in yeast. The Tco89 protein is unique to TORC1 and mTORC1 has DEPTOR and PRAS40 subunits that have no clear yeast homologues. When access to nitrogen is sufficient for the cell, both TORC1 and mTORC are active and localize to the vacuole in yeast or lysosome in mammals[16]. When inactive, TORC1 still localizes to the vacuole, but instead of being dispersed across the entire organelle, the complex is localized to specific puncta on the surface[22]. In a departure from yeast, mTORC1 localizes to the cytosol when inactivated[23]. The change in localization may function as an additional regulator of activity for the complexes. The activation state of

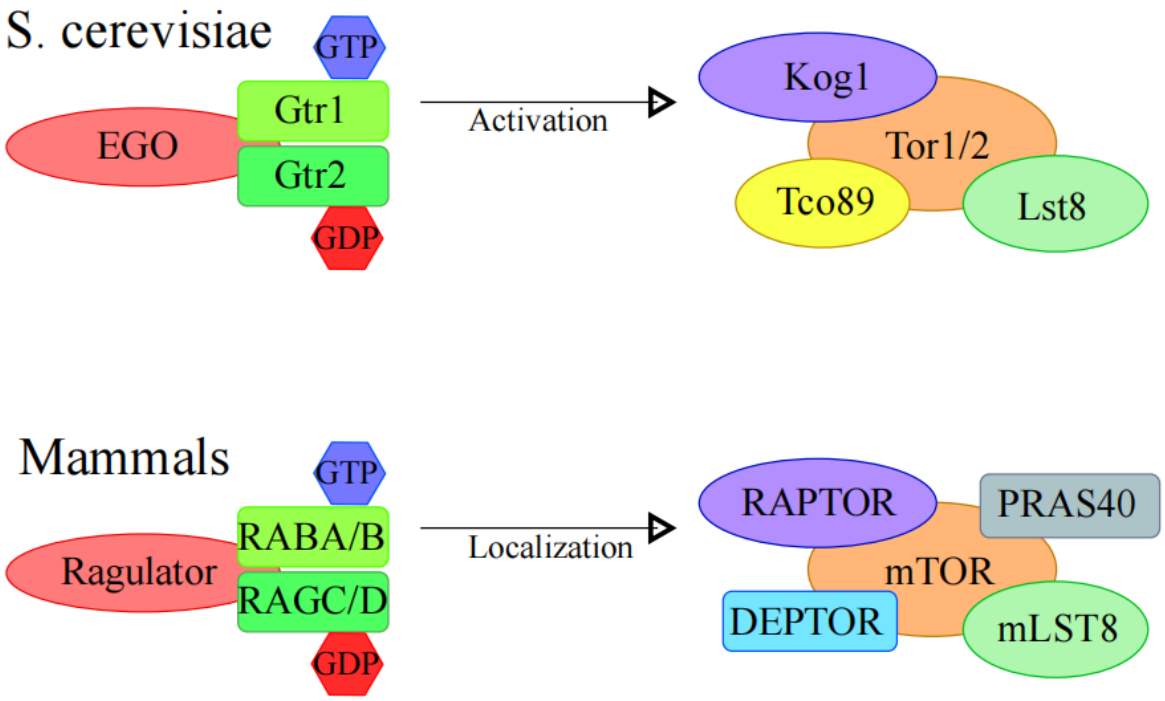


**Figure 1.2: Control of the activation state of TORC1 in S. cerevisiae and in mammals**. A visualization of the EGO/Ragulator complexes in active states interacting with TORC1 complexes in mammals and in yeast. The binding of GTP to Gtr1 keeps TORC1 in its active state on the surface of the vacuole/lysosome. RAGA/B binding to GTP is important for the localization of mTORC1 to the lysosome. Binding of GTP to Gtr2/RAGC/RAGD prevents the binding of GTP to Gtr1/RAGA/RAGB and so prevents the activation of the TORC1 complex. Homologous proteins are shown in the same color to show relation.

TORC1 is determined by a heterodimeric complex of two Rag GTPases, Gtr1 and Gtr2. The Gtr1-Gtr2 complex is tethered to the surface of the vacuole by the EGO proteins, Ego1, Ego2, and Ego3, together forming the EGO complex. The Gtr-EGO complex has two states, $Gtr1^{GTP}$-$Gtr2^{GDP}$ keeps TORC1 active and $Gtr1^{GDP}$-$Gtr2^{GTP}$ will inactivate TORC1. Kog1 binds directly to Gtr2, and this binding is necessary for the proper regulation of the activation state of TORC1[24]. The activation state of mTORC1 is determined by four Rag GTPases (RAGA, RAGB, RAGC, and RAGD) localizing to the lysosome. On the lysosome the ragulator complex, an ortholog of the EGO complex, tethers the Rag GTPases to the surface. Similarly to yeast, the Rag GTPases form a heterodimer where RAGA or RAGB dimerizes with RAGC or RAGD. The complex has an active form of $RAGA/B^{GTP}$-$RAGC/D^{GDP}$ and an inactive form of $RAGA/B^{GDP}$-$RAGC/D^{GTP}$. mTORC1 is recruited to the active RAG heterodimer by the RAPTOR subunit[25]. The nucleotide-binding state of RAGA/B-RAGC/D regulates the localization of mTORC1, once localized to the lysosome it is activated by a small GTPase called RHEB. A comparison between the two complexes can be seen in figure 1.2. Because of the structure of the Gtr1-Gtr2 and the RAGA/B-RAGC/D heterodimer, the

binding of GTP to one subunit in the dimer causes a conformational change which prevents binding of GTP to the other.

The variety of different functions in TORC1 means that it responds to many different signals including nutrient availability, but also oxidative stress on the cell, heat responses, and hypoxia. Given the seriousness of the signals, the response must be adaptive and closely regulated. The response to nitrogen starvation in the cell is the deactivation of TORC1 which has many effects on the cell including the entry into autophagy. The mechanisms regulating TORC1 and mTORC1 activity will be explored later in the paper.

## 1.3.2 Ras/cAMP/PKA pathway: A parallel control mechanism of autophagy

Autophagy that is initiated by a lack of access to nitrogen is controlled by the TORC1 complex, but this is not the only stimulus that can induce autophagy. In addition to TORC1, the PKA pathway is a regulatory mechanism of the autophagic process in yeast. While TORC1 is sensitive to nitrogen sources, specifically amino acids, the Ras/cAMP/PKA pathway is sensitive to the availability of glucose. PKA is a tetramer with three activating subunits and one regulatory subunit. It regulates autophagy by phosphorylating Atg13 on a separate site from TORC1[26] and by phosphorylating Atg1 preventing its localization to the PAS. The activity of PKA is regulated by Ras GTPases. Yeast has two Ras GTPases, Ras1 and Ras2, both of which become active in the presence of glucose, $Ras^{GTP}$ is the active forms of the proteins whereas $Ras^{GDP}$ is the inactive form. When glucose is present, the proteins shift to an active form and activate a adenylate cyclase, Cyr1 thus synthesizing cyclic AMP (cAMP), a second messenger serving several functions in the cell. When the regulatory subunit of PKA, Bcy1 is bound by cAMP it becomes inactivated which is necessary for PKA activity. A drop in cAMP causes an inactivation of PKA and decreased phosphorylation of Atg1 and Atg13. The inactivation of PKA has been shown to be enough to trigger autophagy[27] in some cases. This paper will largely focus on nitrogen starvation as an inducing signal for the cell to enter autophagy and so will not focus more on PKA.

## 1.4 Core machinery and process of autophagy

The work of Ohsumi and many after him have explored the mechanisms of autophagy and so the system is generally well understood. The mechanical process of autophagy can be divided into three main phases, the initiation, autophagosome synthesis, and degradation. The initiation of autophagy begins with the inactivation of the TORC1 complex, which signals to the cell that there is a reduction in the availability of nutrient sources. Atg13 is a major downstream target of TORC1 and while TORC1 remains active it is kept hyperphosphorylated, which inhibits the entry into autophagy[28]. Once nutrient sources run low and TORC1 is inactivated Atg13 is rapidly, but partially, dephosphorylated. This allows the formation of an active complex with Atg1 as seen in figure 1.3. The formation of the Atg1-Atg13 complex appears to be necessary for the formation of a bigger complex with the Atg17-Atg31-Atg29 complex. The combination of the two protein complexes results in the Atg1-Atg13-Atg17-Atg31-Atg29 complex, hereby referred to as the Atg1 complex. The formation of the Atg1 complex is generally thought to mark the initiation of autophagy. The mammalian counterpart to the Atg1 complex is the ULK1 complex which also contains a homolog of Atg13 and an ortholog of Atg17. Functionally, the Atg1/ULK1 complex acts as a scaffold that can bind other Atg proteins and on which the autophagosome can be formed[29]. Atg1 binding to Atg13 and Atg17 also seems to be necessary for Atg1 kinase activity important for autophagy[30]. If the kinase activity of Atg1 is specifically knocked out the number and size of autophagic bodies in the vacuole decreases significantly. It does not remove them entirely as an Atg1 mutant would do, indicating that the role of Atg1 in autophagy is not limited to its kinase activity. Once assembled the Atg1 complex localizes to the phagophore assembly site (PAS), sometimes called the pre-autophagosomal structure, on the vacuole. The ULK1 complex localizes to the mammalian equivalent of the PAS which is the omegasome. Notably, the omegasome does not localize to the lysosome.

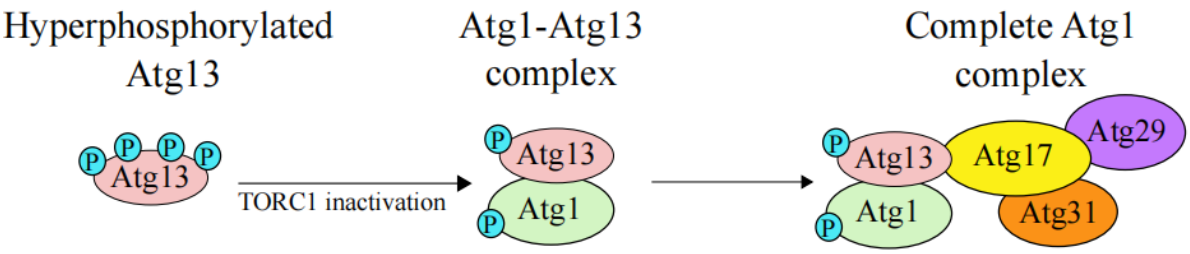


**Figure 1.3: The three-step formation of the Atg1 complex**. A simple visualization of the process which initiates autophagy. Hyperphosphorylated Atg13 is unable to bind to Atg1, upon deactivation of TORC1 the phosphorylation of Atg13 stops and it is partially dephosphorylated. Atg13 forms the Atg13-Atg1 complex which in turn attracts the Atg17-Atg31-Atg29 complex which is constitutively formed in the cytosol. The complete Atg1 complex localizes to the PAS on the vacuole and functions as a scaffold for the phagophore.

## 1.4.1 Formation of the autophagosome

Autophagosome synthesis begins with the elongation of the double membraned phagophore around the cargo. Elongation requires to the recruitment of membrane to the PAS, a process that is not fully understood, but is generally thought to involve Atg9. Atg9 is a transmembrane protein in complex with Atg27 and Atg23[31] found in mobile vesicles called Atg9 vesicles that seem to be derived at least in part from the Golgi apparatus in yeast[32]. These vesicles are found to transit between cytosolic puncta and the PAS at the elongation step and a fraction of the membrane of the autophagosome does contain membrane recruited from Atg9 vesicles. The function of the cycling of Atg9 to the PAS is not entirely clear, but recent work indicates that it functions as a nucleating event with the membrane functioning as a seed membrane for the phagophore[33]. This would allow contact sites with other organelles that can help feed lipids into the membrane, particularly the ER. It would appear that mAtg9 functions together with the ULK1 complex in a similar fashion[34] using mAtg9 vesicles as seed membranes. At the stage of nucleation, the phosphatidylinositol-3 kinase complex I (PtdIns3K) binds to the PAS and produces phosphatidylinositol 3-phosphate (PI(3)P). The ubiquitin-like protein Atg8 is conjugated to PI(3)P by two complexes, first binding to Atg7-Atg3 and then being transferred from Atg3 to PI(3)P by E3 ligase activity from Atg12-Atg5 to form Atg8-PE[35]. It has been suggested that Atg8-PE is responsible for membrane curvature in the autophagosome, thus helping direct the size and shape of the autophagosome as well as for cargo selection in selective autophagy[36]. Once elongated the phagophore closes off and becomes the autophagosome. The majority of the Atg protein machinery dissociates from the

autophagosome either before it is complete or directly after[28]. Atg8 is dispersed equally on both the inner and outer membrane of the autophagosome, but before it can leave the PAS the Atg8-PE on the outer membrane is cleaved off by Atg4 in a process essential for the progression to vacuolar degradation. Notably, Atg8 on the inner membrane remains as the autophagosome is fused with the vacuole which makes it useful for tracking autophagosomes and their fusion into the vacuole.

### 1.4.2 Vacuolar targeting, fusion, and degradation

After completion of the autophagosome it is targeted to vacuole for degradation in yeast. The PAS localizes to the vacuole, but the autophagosome must still be tethered and fused into the vacuolar membrane. Tethering happens through the Rab GTPase Ypt7 and the HOPS (Homotypic fusion and vacuole protein sorting) complex. Once tethered, fusion is facilitated by SNARE proteins, specifically Ykt6 on the autophagosome and Vam3, Vam7, and Vti1 on the vacuole. The outer membrane of the autophagosome fuses with the vacuole and the inner membrane becomes an autophagic body inside the vacuole. Because the omegasome does not localize to the lysosome, the completed autophagosome must be transported to the lysosome. This transport appears to happen across microtubules with the aid of the dynein motor protein[37]. For the vacuole to have access to the cargo inside the autophagic body the membrane must be broken down, a process depending on the lipase Atg15 as well as some hydrolases[28]. Cargo from the autophagosome is then broken down by the acidity of vacuole and the vacuolar hydrolases and proteinases present inside. The products of the degradation are transported out of the vacuole by vacuolar transporters and are available to the cell for re-use.

## 1.5 TORC1 activity as regulated by nitrogen sensing

Autophagy is an adaptive response to the changes in nutritional access in the cell initiated by the dephosphorylation of TORC1. The activation of the autophagy response is therefore dependent on precise information about the cell’s access to nutrition, specifically nitrogen sources. This information is mainly transmitted to TORC1 by guanine nucleotide exchange factors (GEFs) and GTPase-activating proteins (GAPs). GEFs and GAPs act on the EGO complex to change the GTP binding states of Gtr1-Gtr2. GEF proteins will remove a GDP bound to Gtr1 allowing it to bind with GTP and shift into an active state whereas GAP

proteins will active GTPase activity in Gtr1 which causes the bound GTP to change to GDP and thereby terminate the activity of the protein.

Several pathways have been found that the Gtr-EGO complex could potentially use to sense the amino acid levels in the cell and thereby its nitrogen content[38]. Vam6 is a GEF protein regulating of the GTP binding of Gtr1, it is also a part of HOPS complex that tethers autophagosomes to the vacuole[20]. Vam6 shifts Gtr1 into its active state thereby keeping TORC1 active and it seems to do this in an amino acid sensitive manner. L-leucyl-tRNA synthetase (LeuRS) has also been suggested as a signaling mechanism keeping TORC1 active[39]. LeuRS is responsible for the attachment of leucine to its complementary tRNA molecule. The theory is that it functions as a sensor for leucine availability in the cell and interact directly with Gtr1 to signal availability. SEACIT (Seh1-Associated Complex Inhibiting TORC1) is a complex that functions as a GAP om Gtr1 inhibiting TORC1 activity. SEACIT has been shown to be active when the cell is deprived of leucine[40]. The function of the SEACIT complex is evolutionarily conserved to mammals in the GATOR1 (Gap Activity TOwards Rags1) complex. SEACAT (Seh1-Associated Complex Activating TORC1) has been found to inhibit SEACIT activity and upregulates TORC1 activity. Recent work indicates that the role of SEACAT might be as a scaffold on which other nutrient sensors bind to regulate the activity of SEACIT[41]. The mammalian equivalent to SEACAT is GATOR2 which has some theorized regulators. SESTRIN2 binds to leucine when it is present in the cell. If there is a deficit of leucine it is theorized that SESTRIN2 will bind to GATOR2 instead preventing from localizing to the cytosol[42]. The exact mechanism of SESTRIN2 and GATOR2 binding and regulation is not fully understood. In response to arginine starvation, the protein CASTOR1 inhibit its GATOR2 activity[43]. Notably, yeast does not have a SESTRIN2 or CASTOR1 ortholog, so this is not a conserved regulatory mechanism. As described above, there are some unanswered questions regarding how information is transferred to RAG GTPases and many alternate sources of information in addition to the lysosome/ vacuole and the cytosol are suggested including from the plasma membrane and the mitochondria[19]. The introduction of autophagy in yeast is especially sensitive to the levels of glutamine. In both yeast and mammals, glutamine has been found to activate TORC1 in the absence of the Gtr-EGO complex. While the mechanism is not fully understood, it is believed to involve Pib2, a vacuolar membrane-associated phosphatidylinositol 3-phosphate binding protein and a Vps34-Vps15 phosphatidyl 3-kinase complex[44]. The mechanism of this glutamine sensing appears to be dependent only on machinery found in the vacuole[45].

The many regulatory pathways for TORC1 in response to specific amino acid availability displays its function as an extremely finely tuned regulator of the cellular response to nutrient starvation.

## 1.6 Memory is an adaptive response to changing environments

Cell memory is a function by which a cell retains information about its previous conditions and uses that information to adapt more rapidly should similar conditions recur. The retention of information allows a cell to adapt to both changing and cyclical environments by reactivating a previous state or process. Transcriptional memory is an evolutionarily conserved ability seen across a diverse set of organisms, from yeast, to plants, to mammals. Yeast is one of the organisms most suited to the exploration of memory because of its simple genome and relatively simple regulatory mechanisms. As of yet, no memory mechanism has been examined in the process of autophagy, however several other mechanisms of memory have been discovered and there are some similarities found across them that could give an indication of what the process would look like in autophagy. The reactivation of INO1 is a system of memory that is well explored[46], similarly GAL gene reactivation has given many insights into the process[47]. Both INO1 and the GAL genes are expressed in response to nutritional changes and memory is formed and reactivated in response to these changes.

The information about previous experiences can persist over several generations of cells so that even daughter cells with no experience with the stimulus can show adaptive behavior[48] thus allowing adaptation across generations. Generally, memory is retained epigenetically through the manipulation of chromatin[49], which can be aided by the retention of cytosolic components[47] that are useful in response to reactivation. This form of memory is not permanent, and memory will be lost over time unless the cell is re-exposed to the original stimulus. The time it takes for memory to be lost appears to be dependent on the genes being expressed and the strength of the stimulus, but in some cases, memory can be retained for 12 hours or more.

## 1.6.1 Mechanisms of chromatin-based memory

Once a gene has been transcribed in response to certain stimulus, it can in some cases be primed for reactivation by an alteration in the chromatin structure around that gene. The mechanisms of this process can vary between genes and not all genes can be primed for reactivation, however the process does appear to have some common elements. To begin, memory seems to require a DNA sequence in the promoter known as a memory recruitment sequence (MRS) that can be recognized by transcription factors[46]. Once the transcription factor is bound, the gene locus is moved to the nuclear periphery near the nuclear pore complex (NPC)[50]. Continued localization to the NPC is essential for memory and the function of the MRS appears to be to maintain this localization after gene expression is repressed.

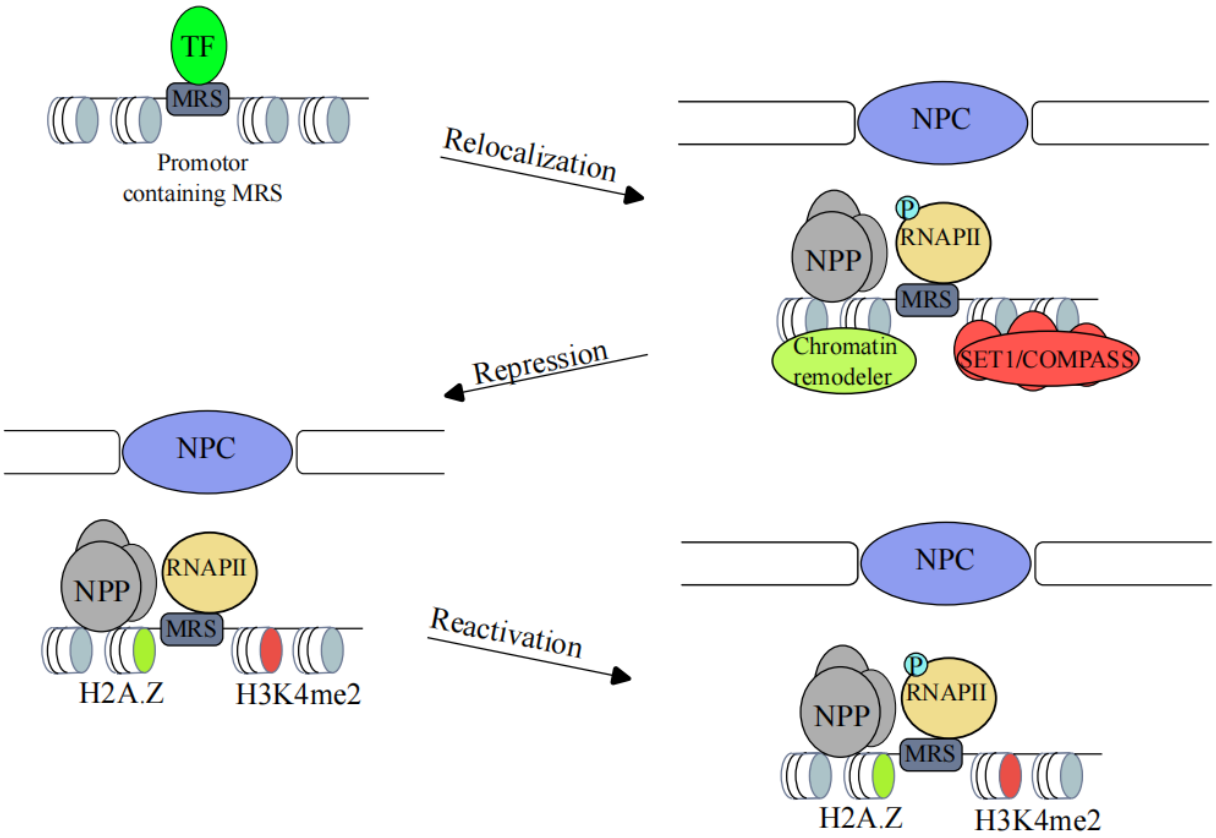


**Figure 1.4: A model of chromatin-based memory.** Binding of a transcription factor to the promoter leads to relocation to the nuclear pore complex (NPC) in the nuclear membrane. Nuclear Pore Proteins (NPP) stabilize the localization to the NPC. The presence of a memory recruitment sequence (MRS) in the promoter leads to remodeling of the chromatin around the promoter sequence with the canonical histone H2A being replaced with H2A.Z and the SET1/COMPASS complex performing H3K4 dimethylation. Following repression of the gene, a poised, but not actively transcribing, RNAPII is recruited to the promoter. When the cell resumes signaling for the expression of the gene, the reactivation the RNAPII will begin transcription without the time-consuming step of binding to the target gene. The presence of memory requires active maintenance of this chromatin state, both in localization and the changes in histone structure.

Notably, mutation of the MRS has no effect on the initial transcription rate of the gene but will reduce the reactivation rate[51]. In INO1 the continued localization to the nuclear periphery depends on the activity of nuclear pore proteins like Nup100, but this is not universal. Other genes, including the GAL gene cluster use intragenic loops formed between the promotor and 3' end of the gene to maintain localization to the NPC[52]. the demethylation of histone H3 lysine 4 (H3K4) at the promoter sequence of the gene seems to be a universal trait of chromatin-based memory. This histone mark is inherited through cell division, thus allowing for multigenerational memory. Methylation of H3K4 is performed by the SET1/COMPASS complex[53] in yeast, whereas multiple complexes are responsible for the process in higher eukaryotes[54]. Replacing canonical histones with non-canonical versions is also a form of chromatin remodeling essential to the process. Histone H2A.Z is has been found to play a part in transcriptional regulation[55] and is essential in several memory formation process discovered so far[56]. Without H2A.Z, neither GAL genes or INO1 retains localization to the NPC, nor do they show rapid reactivation. The insertion of H2A.Z seems to be at least partially dependent on the MRS being present in the promoter and on the SWRC1 complex[57]. Another important protein in the expression of memory is SWI/SNF, it is an ATP-dependent chromatin remodeler that displaces H2A and H2B histone subunits from nearby histones. This mechanism is essential for the expression of some forms of GAL gene memory[58]. Cytosolic components can also help to reactivate the cell in response to a change in cell signals. Notably, in a heterokaryon experiment where Gal1 was present in the cytosol, but the chromatin modifications were not, the cells still expressed transcriptional memory[59]. On the other hand, the SWI/SNF chromatin remodeling complex is essential for GAL gene memory expression showing that an interplay between cytosolic components and chromatin remodeling still occurs.

The mechanism of chromatin-based memory appears to be keeping RNA polymerase II (RNAPII) poised at the gene in an inactive state, allowing the cell to rapidly re-initiate transcription if the signal to do so recurs[51]. When recruited in this form, the C-terminus of RNAPII is not phosphorylated, keeping the enzyme from entering transcription. The machinery binding RNAPII for the first binding and the machinery docking RNAPII to prepare for the second activation are similar, but the docking of RNAPII requires a Cdk8 mediator and not Cdk7[53]. In short, chromatin-based memory requires an MRS sequence in

the promoter that causes chromatin be organized in such a way that the gene is localized continuously to the NPC, it must then be bound by an RNAPII that is poised for reactivation.

### 1.6.2 Prions and prion-like proteins and their role in memory

There are other processes for memory outside of chromatin-based mechanisms. The role of prions in yeast transcriptional memory has not been fully elucidated, but they have been found to have some memory effect[60]. Prions are self-propagating proteins that spread their specific fold-structure onto other proteins and so accumulate. In mammals, prions are considered pathogenic and are linked to many neurogenerative diseases. The role of prions in yeast is less straightforward with some forms being lethal while other forms are only slightly harmful and some are hypothesized to be functional in the cell[61]. Prions form stable cross-beta-sheet amyloid fibers which can be from which prion seed templates can be cleaved by the Hsp104, a protein remodeling factor. These seeds can be transferred from mother cell to daughter cell, spreading the prion[62]. Research on heat stress saw that the transition of Lsb2 into a prionic form, [$LSB^{+}$], coincided with an increased thermotolerance and that the prion could remain in a fraction of the cells for several generations[60]. Many genes can display a prion-like inheritance pattern upon overexpression without the formation of amyloids and these can have beneficial effects for generations[63]. While these proteins do not form amyloids, they still have evolutionarily conserved disorganized domains that are also found in prions. The role of prions and prion-like proteins in the cellular function of yeast is controversial, and much work is still needed to explore the subject, but it represents a potential mechanism of memory that warrants further examination.

## 1.7 Using *Saccharomyces cerevisiae* as a model organism

Much of the research within both autophagy and memory has been conducted using S. cerevisiae as a model organism. The autophagy core machinery found by Yoshinori Ohsumi was discovered specifically with *S. Cerevisiae* as a model[2] and early discoveries in transcriptional memory were done in yeast. There are many base cellular functions that are evolutionarily conserved between yeast and higher eukaryotes including humans and

discoveries in yeast have been extremely important to guide the research in higher eukaryotes. *S. cerevisiae* is also a convenient organism to work with because it has a short generation time and few to no ethical concerns making planning and execution of experiments very straightforward. Furthermore, because *S. cerevisiae* is a single-celled organism it is possible to draw conclusions about cellular functions without having to account for regulatory mechanisms coming from other parts of the organism. It is also possible to precisely control the nutritional access and growth rate of yeast to fine-tune experiments precisely. The relatively small genome of *S. cerevisiae* and the relative lack of introns also means that it has a well explored genome with many genes being characterized[64]. Several decisions made during the execution of experiments in this paper are based on whole genome screens that would be difficult to execute in other organisms (Enserink lab, unpublished data). The simplicity of the organism both in terms of experimental procedure and genome also has allowed for a great deal of work to be done in systems biology using *S. cerevisiae* which has in turn been extremely useful for our understanding of cellular processes and diseases in humans[65]. In this paper the terms *S. cerevisiae* and yeast are both used and unless otherwise specified refer to the same organism.

# Chapter 2

# Aims of the project

The objective of this project is to examine the effect of previous exposure to nitrogen starvation on the autophagy response in the cell in order to gain an understanding of the effect of memory in the autophagic response and to find potential regulatory mechanisms of this effect. There are two essential questions that are addressed, 1) Does *S. cerevisiae* display a memory effect in autophagy when repeatedly exposed to nitrogen starvation and how long a starvation period is needed before this effect becomes apparent in the response? 2) Are there specific proteins that serve as a regulatory mechanism of this effect and if there are how does this regulation occur?

To answer these questions, we imaged WT strain *S. cerevisiae* through a cycle of nitrogen starvation, replenishment, and a second phase of nitrogen starvation. When imaging through this cycle we varied the initial starvation period and replenishment to examine changes in the phenotype. Using information about timing from the initial experiments we executed a large-scale screening of single-deletion mutants selected based on characteristics of their autophagy response and GO terms relevant to autophagy.

# Chapter 3

# Methods

## 3.1 Yeast strains used in the experiments

The experiments all utilized different strains of *Saccharomyces cerevisiae*. In the initial study of autophagic memory WT strains were used. They were grown in complete supplement mixture or CSM (Formedia, Hunstanton, UK)(complete content), a complete minimal media. At set points in the experiment the cultures were transferred to synthetic dropout -nitrogen or SD-N (Formedia, Hunston, UK) (complete content), a media lacking amino acids, ammonium sulphate, or any other nitrogen source. A screen was performed with preselected mutants (Table 3.1), grown in the same media. For the autophagic memory experiments and screen the yeast was grown to the exponential phase at the start of the experiment. Western blot experiments used two different strains, one grown in CSM without leucine, and another grown in CSM. Both strains were at a point shifted to SD-N. In the western blot experiments the yeast was grown to a mid-exponential phase.

## 3.2 Study of autophagic memory

The examination of potential memory effects was executed by imaging WT strains of yeast through cycles of starvation and replenishment using live cell high throughput microscopy. The examination was done in two stages. In the first stage of experiments the initial starvation phase was varied between 1 and 8 hours, the replenishment was 4 hours, and the second starvation was 12 hours. The second stage used three different initial starvation times, 1 hour, 4 hours and 8 hours. In this experiment replenishment was extended to 7 hours and the second starvation was 12 hours. Relevant wells were imaged once per hour. All strains used in this experiment contain two specific genetic reporters, nG-Atg8 and Pep4-mCherry. Atg8 locates to the autophagosome and Pep4 to the vacuole. By tracking both reporters, we tracked the

autophagic state of a given cell. The images from the microscope were analyzed using a semi-supervised machine learning approach to image analysis (see figure 3.1 for an overview).

## 3.2.1 Preparation of master plates

To properly store strains between experiments a master plate containing all relevant strains was made before the first experiment. The strains were collected from a -80 °C freezer at the Enserink lab. The master was made in 96-well clear plates. Strains were inoculated into 150µl of CSM and grown for 3 days in an incubator at 25°C. This methodology was also used for the screen. In the study of autophagic memory 1µl was used to incubate, in the screen certain mutants were slow growers and needed 4µl, see table 3.1 for quantities for each specific mutant. To protect the integrity of the cells at -80 °C, 50µl of 80% glycerol was added to each well and the wells were resuspended. The plate was covered with a plastic film to prevent evaporation during the freezing process.

## 3.2.2 Coating of plates used for imaging

To fix cells for imaging, 96 Well Black/Clear Flat Bottom TC-treated microplates (Corning, Corning, NY) were treated with 60 ml of previously unused concanavalin A 0.25 mg/ml for one hour. The concanavalin A was then removed and kept for reuse in other experiments. Reuse of old concanavalin in these experiments lead to a reduced ability to fix cells to the bottom of the plate for the duration of the experiment. The coated plates were sealed in plastic bags and kept at 4 °C for up to 4 days until it was time to inoculate them with the relevant yeast strains.

## 3.2.3 Preparation of the strains and the plate for high-content imaging

To remove any latent memory effects and ensure the strains were growing correctly, the strains were first grown and reinoculated through cycles. Four days before imaging the master plate was removed from storage at-80 °C and thawed for around two hours. The strains were

resuspended and inoculated onto a new plate according to a layout determined by the specific experiment. Because the plate is imaged through a timelapse, none of the outer wells in the plate were used as this could disrupt the focus of the microscope. In each relevant well 1µl of strain was inoculated into 200µl of CSM. The plate was then incubated for 48 hours at 25 °C in a container to maintain humidity. After 48 hours the wells were all checked for growth. If the cells were growing normally a new plate was inoculated with 1µl of relevant strain into 200µl of CSM. The new plate was inoculated for 24 hours. The final incubation period was only 12 hours long. For this reason, the volume of strain inoculated at this step was 4µl into 200µl of CSM. This was inoculated on the treated black plate. To properly distribute the cells on the bottom of the plate, the wells were gently resuspended after inoculation. The volume resuspended was 10µl and it was done 5 times in 5 locations in the well (center and four sides), taking care not to touch the bottom surface of the well to avoid any disruption of the concanavalin. The black plates were incubated for 12 hours at 25 °C. When the cells were transported, they were covered with a plastic film. Before imaging the media was removed from all the wells. If the wells weren't set to be imaged at the start of the experiment, 200µl of fresh CSM was added. This ensures that the cells do not go into autophagy because the media was consumed. If the well was set to be imaged at the start of the experiment 200µl of autoclaved mq$H_2O$ was gently added and then removed twice to wash away any residual CSM which would prevent the cells going into autophagy. 200µl SD-N was added to the washed wells and the plate was ready for imaging.

## 3.2.4 Live cell high-content microscopy

The microscope used was the ImageXpress Micro Confocal High-Content Imaging System (Molecular devices, San Jose, CA). To ensure that the temperature was stable at the start of the experiment, the temperature of the microscope was set to 25 °C the day before the imaging. The microscope imaged three sites in all relevant wells once per hour every hour of the experiment. Each site was imaged at three different wavelengths simultaneously. The FITC filter was used at 200 ms exposure, Texas red at 800 ms, and TL 50 at 10 ms. This allowed the tracking of Atg8, Pep4, and the cell surface simultaneously. Before imaging the cells were checked for normal growth and any potential artefacts. To ensure proper focus the offset was adjusted for each filter and saved as a template file. At the start of the experiment

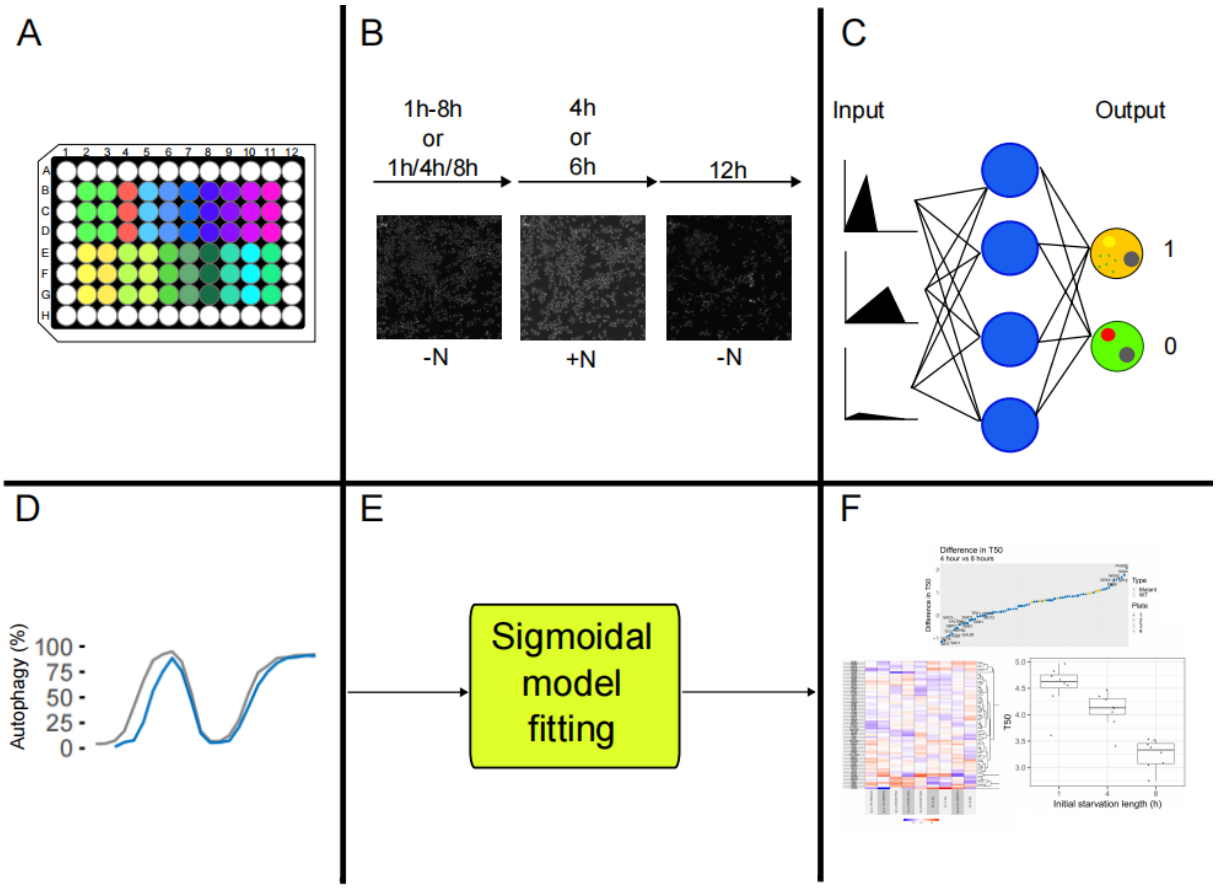


**Figure 3.1 General pipeline for the live-cell imaging experiments.** The pipeline for examining potential memory effects in the autophagy response in S. cerevisiae grown through cycles of starvation and replenishment using techniques developed at the Enserink lab. **(A)** The initial study of autophagy used WT strains to examine autophagy response whereas the screen used two WT strains, an Atg1Δ strain and 17 mutants. The layout in the workflow is from the screen. These were prepared through cycles of growing in complete supplement mixture (CSM) to remove any latent memories. **(B)** To image the cells through cycles of autophagy, they were transferred to a synthetic minimal media (SD -N) for varying lengths of time. The cells were then transferred to CSM and imaged for 4/6 hours depending on experimental protocol. They were then transferred back to SDN and imaged for another 12 hours. **(C)** The images from the microscopy experiment were analyzed using a semi-supervised machine learning approach developed at the Enserink lab. Using this approach each cell was classified as either inducing autophagy (1) or non-autophagy inducing (0). **(D)** The data from the classified cells was used to predict the percentage of cells in autophagy in each well. **(E)** A sigmoidal model was fitted to the data from the predictions and relevant parameters of the sigmoidal curves was extracted for. **(F)** Further analysis was done on the extracted parameters of the sigmoidal models.

and at specific times in the experiment the cells were transferred to new media. If they were transferred from SD-N to CSM, the wells were simply emptied of media and new media was added. If the cells were transferred from CSM to SD-N they were washed in the way described in plate preparation. During the replenishment and second starvation steps of the experiment the plate was imaged automatically using the time lapse function of the microscope, still imaging the same sites once per hour.

### 3.2.5 Data analysis of live cell high-content imaging

Tracking the Atg8, Pep4, and the cell surface with the images from the microscope allowed the categorization of each cell into autophagy or not. Using a machine learning approach to image analysis developed at the Enserink lab, each cell was grouped as in autophagy, represented by 1, or not in autophagy, represented by 0. The quantification was executed using a semi-supervised machine learning approach in an automatic pipeline developed in Fiji. Using data from the quantifications the percentage of cells in autophagy in each given well was predicted using a pipeline in R. To examine whether there is a learning effect a sigmoidal model was fitted to the responses from second starvation phase using the R package SICEGAR v 0.2.4. By fitting the model, we could extract parameters of interest for the study. The parameters of interest were Autophagy max, the highest level of autophagy reached, the slope of the sigmoidal curve, and the T50, the time it takes to reach halfway to the max level of autophagy. Parameters were extracted from each individual well in the experiment and compared using the geom_box function of ggplot2.

## 3.3 Large-scale screen for memory-related mutants

The methodology for the screen utilized many of the same techniques as were applied in the study of autophagic memory. The material differences being that a list of pre-selected mutants were screened instead of just WT strains and there were some notable differences in analysis. The mutants were chosen based on the kinetics extracted from a Genome-wide autophagy screen previously executed at the Enserink lab. Using analysis made on the results of this screen, specific criteria were used to select mutants for the experiment. The mutant displayed a disruption in autophagy (FDR>0.05 for A_Start/A_max/A_final), they could have a lower

max autophagy, but their autophagy induction prediction must be sigmoidal (FDR>0.05 for A_Start/A_final/log_likelihood), and they ccould have a higher initial autophagy (FDR>0.05 for A_max/A_final). Each criterion also had a FDR<0.01 for slope and FDR<0.1 for T50 ensuring fidelity in those parameters. The parameters were further narrowed down by filtering for relevant GO categories, namely Signaling, Transcription, Translation, mRNA processing, and Chromatin remodeling. This resulted in a list of 66 mutants of interest (table 3.1). The strains were collected from the yeast knockout collection[66] or the decreased abundance mRNA perturbation collection, both stored at -80°C in the Enserink lab. Certain strains had a greater inhibition in growth and so were inoculated at a greater volume to ensure growth as noted in table 3.1. Inoculation volume onto the black plate was 3 µl for the normally growing strains and 5 µl for the slow growers. Beyond that every plate was prepared as described in3.2.3 Preparation of the strains and the plate for high-content imaging. The mutants were distributed across 4 unique plates, each with 17 mutant strains, two WT strains and one strain of *atg1Δ* functioning as a negative control. Each strain was grown with three initial starvation times, 1 hour, 4 hours, and 8 hours with a replenishment period of 4 hours and a second starvation period of 12 hours. The cells were imaged using the same methodology as described in 3.2.4 Live cell high-content microscopy.

Table 3.1: **Mutants used in the screen:** A list of all mutants used in the screen, including Gene, ORF, Type and the volume inoculated during early incubation.

| Gene | ORF | Library | Volume inoculated |
|---|---|---|---|
| TFC7 | YOR110W | DaMP | 1 ul |
| POB3 | YML069W | DaMP | 4 ul |
| DEP1 | YAL013W | KO | 1 ul |
| CCR4 | YAL021C | KO | 1 ul |
| GPB2 | YAL056W | KO | 1 ul |
| SWC3 | YAL011W | KO | 1 ul |
| SWD3 | YBR175W | KO | 1 ul |
| DPB4 | YDR121W | KO | 1 ul |
| KIN1 | YDR122W | KO | 1 ul |
| NPL3 | YDR432W | KO | 4 ul |
| PTP3 | YER075C | KO | 1 ul |

Continued on the next page

**Table 3.1: Mutants used in the screen**

| Gene | ORF | Library | Volume inoculated |
|---|---|---|---|
| KSP1 | YHR082C | KO | 1 ul |
| GBP2 | YCL011C | KO | 4 ul |
| IXR1 | YKL032C | KO | 1 ul |
| VMA5 | YKL080W | KO | 1 ul |
| INP53 | YOR109W | KO | 1 ul |
| RME1 | YGR044C | KO | 1 ul |
| ARP6 | YLR085C | KO | 1 ul |
| SFL1 | YOR140W | KO | 1 ul |
| HAL5 | YJL165C | KO | 1 ul |
| SWI3 | YJL176C | KO | 4 ul |
| TPK1 | YJL164C | KO | 1 ul |
| SAC3 | YDR159W | KO | 4 ul |
| GCN1 | YGL195W | KO | 1 ul |
| RTF1 | YGL244W | KO | 1 ul |
| SSN3 | YPL042C | KO | 4 ul |
| CKB1 | YGL019W | KO | 1 ul |
| GCR2 | YNL199C | KO | 1 ul |
| URE2 | YNL229C | KO | 1 ul |
| SAC1 | YKL212W | KO | 4 ul |
| GAL80 | YML051W | KO | 4 ul |
| SWR1 | YDR334W | KO | 1 ul |
| MOT3 | YMR070W | KO | 1 ul |
| MGA2 | YIR033W | KO | 4 ul |
| ASF1 | YJL115W | KO | 4 ul |
| SRB2 | YHR041C | KO | 4 ul |
| RSF2 | YJR127C | KO | 1 ul |
| PTC6 | YCR079W | KO | 4 ul |
| REG1 | YDR028C | KO | 1 ul |
| SRB8 | YCR081W | KO | 4 ul |
| SSN8 | YNL025C | KO | 1 ul |

Continued on the next page

**Table 3.1: Mutants used in the screen**

| Gene | ORF | Library | Volume inoculated |
|---|---|---|---|
| FKH2 | YNL068C | KO | 1 ul |
| CGI121 | YML036W | KO | 4 ul |
| VPS71 | YML041C | KO | 1 ul |
| ATG14 | YBR128C | KO | 1 ul |
| PKH3 | YDR466W | KO | 1 ul |
| SNF4 | YGL115W | KO | 1 ul |
| VPS72 | YDR485C | KO | 1 ul |
| SSN2 | YDR443C | KO | 1 ul |
| CHD1 | YER164W | KO | 1 ul |
| GRX4 | YER174C | KO | 4 ul |
| SPT2 | YER161C | KO | 1 ul |
| RIM15 | YFL033C | KO | 1 ul |
| HST3 | YOR025W | KO | 1 ul |
| CKB2 | YOR039W | KO | 1 ul |
| GPB1 | YOR371C | KO | 1 ul |
| PHO80 | YOL001W | KO | 1 ul |
| HTZ1 | YOL012C | KO | 4 ul |
| VMA4 | YOR332W | KO | 4 ul |
| GCN5 | YGR252W | KO | 1 ul |
| HTB2 | YBL002W | KO | 1 ul |
| SUS1 | YBR111W-A | KO | 1 ul |
| SCH9 | YHR205W | KO | 1 ul |
| - | YPL150W | KO | 1 ul |
| STH1 | YIL126W | DaMP | 1 ul |
| RPC34 | YNR003C | DaMP | 4 ul |

## 3.3.1 Analysis of the memory screen

The process used to quantify and classify the cells was the same as the one used in section 3.2.5 Data analysis of live cell high-content imaging. The SICEGAR package v 0.2.4 in R

was used to extract parameters. The extracted parameters were used to reconstruct the curves so as to clean them and make them easier to inspect. Different initial starvation times for the same strain yielded different parameters, the differences found between parameters were plotted in a set of waterfall plots. The differences were also charted together in a heatmap made with the superheat package v 0.1.0 in R. The heatmap was scaled to mean=0 sd=1 using the scale=TRUE argument.

## 3.4 Western blot assays to examine potential mechanisms of memory

Two sets of biological assays were done to examine the potential biological underpinnings of a memory effect. Both assays were examining the effect through Atg13 in cycles of starvation and replenishment. The first set had a strain with a plasmid containing GFP-Atg13 to examine the phosphorylation state of Atg13. The addition of phosphate groups alters the size of the molecule and therefore its progression through a membrane. The second set had Atg13 with a FLAG tag to examine changes in transcription (see Table 3.2). Both sets had two identical experiments, one experiment with 6 hours of starvation, 4 hours of replenishment, and 12 hours of second starvation and one with the same starvation times and 6 hours of replenishment. In addition, there was one GFP-Atg13 experiment with 8 hours of starvation, 4 hours of replenishment, and 12 hours of second starvation.

Table 3.2: **Genotypical profile of the strains used in western blot experiments**: Relevant information about the WT strains used in the western blot experiments.

| Background | Genotype | Growth media | Source |
|---|---|---|---|
| BY4741[67] | *his3Δ1, leu2Δ0, met15Δ0, ura3Δ0 Pep4-Cherry::hph, NAT-GDP-pr-GFP-ATG8, atg13_5FLAG-KanMX6* | CSM | Enserink lab |
| BY4741 | *his3Δ1, leu2Δ0, met15Δ0, ura3Δ0, plasmid GFP-ATG13* | CSM - Leu | Enserink lab |

To prepare the cells to be assayed they were grown and sampled through an initial starvation phase, a replenishment phase, and a second starvation phase. Because three separate phases are sampled, three separate flasks were prepared and sampled from, one for each phase. To induce starvation the cells were grown in SDN, for replenishment either CSM or CSM -Leu depending on the strain. Once sampled the cells were lysed mechanically using glass beads. The samples were then normalized in volume and separated by gel electrophoresis before being transferred to a membrane. The membranes were visualized for several relevant targets. In both sets of experiments RpS6 phosphorylation was examined to look at TORC1 activity and β-Actin was used as a control.

## 3.4.1 Strain preparation procedure for western blot assays

The relevant strain for the was taken from an 80 °C freezer and thawed. Once ready, the strain was incubated on CSM -Leu or YPD agar plates for three days at 25 °C. Two colonies were collected and inoculated into two 50ml Falcon tubes with 5ml of growth media and were incubated overnight for 16 hours in a shaking incubator at 30 °C. Two 400ml Erlenmeyer flasks with 100ml of relevant growth media were prepared, 5µl of culture was inoculated into one flask, 10µl into the other to ensure growth in at least one flask. The flasks were incubated in a shaking incubator at 30 °C for 6 hours. After the incubation the optical density of both cultures was measured using a Hitachi U-1900 spectrometer (Hitachi High-Tech Science, Chatsworth, CA). Because of the potential for strong growth of the strains in CSM, the samples were diluted to 1:4 before $OD_{600}$ was measured. If both cultures show growth, a culture with an $OD_{600}$ between 0.2 and 0.6 was used or the strain closest to that range if neither were in it. Three 1000ml Erlenmeyer flasks containing 400ml of relevant growth media were inoculated to an adjusted $OD_{600}$ of 0.001. The flasks were put into a shaking incubator at 30 °C and grown for 16 hours.

## 3.4.2 Sample collection protocol

Before starting the experiment, a t0 sample was collected from one of the overnight batches. For the t0, 50ml of culture was collected and run through a filter to remove the media. The

filter containing the cells was then placed in a 2ml Eppendorf tube with 1ml stop buffer to prevent any further reactions in the cells. The tube was vortexed and then the filter was squeezed with tweezers to release any remaining cells from the filter paper before it was discarded. To remove the stop buffer, the tube was centrifuged at 13200 rpm at 4 ℃ for 25 seconds. The supernatant was pipetted out and discarded. The extracted cell sample was then immediately frozen in dry ice. The sample would later be transferred to a -80°C freezer. Later samples collected from the media were 80ml but otherwise they were treated the same way. The sample collected at the end of the replenishment phase was split into two separate 40ml samples, this was to ensure that the high cell concentration after a long growth period wouldn't affect protein extraction. Samples were only collected from one flask in each phase of the experiment. Overall, 18 samples were collected in each experiment. For the specific timing points of sample collection see table 3.3.

Table 3.3: **An overview of timing points for sample collection in the western experiments**: The timing points for sample collection by phase. Certain timing points were dependent on the experiment. In the timepoints with two options the sample was always collected as the other flasks were transferred.

| Phase | Sample Times | | | | | | |
|---|---|---|---|---|---|---|---|
| Before first transfer | T0 | | | | | | |
| Primary starvation | 15' | 30' | 1 hour | 2 hours | 4 hours | 6/8 hours | 12 hours |
| Replenishment | 5' | 10' | 15' | 30' | 1 hour | 4/6 hours | |
| Secondary starvation | 15' | 30' | 1 hour | 12 hours | | | |

## 3.4.3 Growing strains through cycles of starvation and replenishment

Before transfer to SD-N and the beginning of the experiment, the $OD_{600}$ of the three flasks was measured with a Hitachi U-1900 spectrophotometer (Hitchi High-Tech Science, Chatsworth, CA) with a cuvette containing 1ml of CSM as a blank to zero the machine. The samples were diluted to 1:4 to compensate for growth. The adjusted $OD_{600}$ of the culture in the beginning of the experiment should 0.3 in a 560ml volume, using the $OD_{600}$ measured in the overnight batches we could calculate the volume that was needed for that adjusted $OD_{600}$. Before transfer three 1000ml Erlenmeyer flasks with 560ml SDN were prepared. The volume

of culture needed was then filtered through a Millipore vacuum system with a filter capturing the cells. To properly clean the cells of CSM before they went into starvation media 5x the volume of culture filtered of SDN was also run through the system before the filters were removed from the filtering system. To ensure that all three flasks go through the same treatment, the filters were added simultaneously. The flasks were incubated in a shaking incubator with a water bath set to 30°C. Later in the experiment the cells from the two remaining flasks were transferred to 480ml of CSM to induce a replenishment phase. When transferred to CSM there is no adjustment of $OD_{600}$ or cleaning as the cells have not been in growth media and do not need to be cleaned of nitrogen sources, but the process is otherwise the same. To induce second starvation the cells were transferred into 400ml of SDN with an $OD_{600}$ of 0.3, these cells must be washed in 5x volume of culture SDN.

## 3.4.4 Extracting protein from the samples

To begin extraction, the samples were thawed for a few minutes in a steel rack that was kept on ice. Once properly thawed, the cells were resuspended in 1ml 20% TCA. The purpose of the TCA was to precipitate the proteins. The sample was centrifuged at 13200 rpms for 2 minutes and the supernatant was discarded. The sample was resuspended in 1 ml of 1M Tris that was not pH adjusted before being centrifuged for 1 minute at 13200 rpm and discarding the supernatant. This neutralizes the TCA and maintains acceptable pH levels for the p. The pellet was gently resuspended in 100µl 2x sample buffer with 1:10 DTT. To do this the sample tube was dragged along a microtube rack repeatedly until fully resuspended. The DTT keeps the protein unfolded by preventing cysteine side chains from forming disulfide bridges. Once resuspended, the samples were boiled for 2 minutes at 95°C. Glass beads were added to the sample and the sample was vortexed before being boiled for another 2 minutes at 95°C. To break apart the cells mechanically, the samples were run through a Fast-Prep program 4x30 seconds with a 5-minute break between each run wherein the samples were being kept on ice. After the Fast-Prep procedure, the samples were boiled for two minutes at 95°C and then spun down in a minifuge. The sample tubes were pierced at the bottom with a hot needle and put into 15ml Falcon tubes. The Falcon tubes containing the sample tubes were centrifuged using a Kubota 5930 centrifuge (Kubota, Osaka, Japan) for 5 minutes at 3000 rpm. After ensuring that the sample had been transferred to the Falcons, the original sampling tubes containing the glass beads were discarded. The samples were transferred from the

Falcon tubes to new 1,5ml Eppendorf tubes, taking care not to disturb the pellet which is cell detritus that could muddle the assay. The sample was centrifuged once more for 5 minutes at 13200 rpm and the supernatant was transferred to a new 1,5ml Eppendorf tube again taking care to not disturb the pellet. To quantify protein quantity the $OD_{600}$ was measured. Cuvettes were filled with 500µl $H_2O$, 1µl sample and 500µl Bradford 2:3 (2 parts Bradford, 3 parts $H_2O$) and incubated for 5 minutes. A blank was also prepared without sample to zero the spectrometer. By fitting a BSA curve the concentrations of protein in the samples could be calculated. Using the concentration, the volume needed to make sure that each sample contained 30µg was found. The samples were kept in a -80°C freezer.

Table 3.4: **Primary and secondary antibodies used in western blot experiments**: An overview of the antibodies used in in the WB experiments including condition of application of the primary antibody.

| Primary Antibody | Secondary Antibody | Substrate detected | Conditions | Source |
|---|---|---|---|---|
| Anti-Flag (HRP)(monoclonal) | - | FLAG fusion proteins | WB o/n 4°C | Merck (Darmstadt, Germany) |
| Anti-GFP (Polyclonal) | Bovine Anti-Goat | Aequorin | WB 1:1000 o/n 4°C | Abcam (Cambridge, UK) |
| Anti-phospho-RpS6 (Polyclonal) | Anti-Rabbit | Anti-Phospho-(Ser/Thr) Akt Substrate | WB 1:1000 o/n 4°C | Cell Signaling Technology (Danvers, MA) |
| Anti-Actin (Monoclonal) | Anti-mouse | β-Actin | WB 1:1000 o/n 4°C | Abcam (Cambridge, UK) |

## 3.4.5 Gel electrophoresis and membrane transfer

The samples collected previously were thawed on ice and then boiled for 5 minutes at 95°C to prepare them for gel separation. They were then centrifuged for 2 minutes at 13200 rpm. The Bradford assay identified samples that required volumes under 3µl, these were diluted 1:2 with 2xsample buffer 1:10 DTT in a separate tube to ensure they had enough volume to fill their wells. If there was a stark difference in volume required in two adjacent wells one of them might also be diluted to keep the volumes similar. The samples were loaded into two Precast TGX Gel 18 well 4-20% (Bio-Rad, Hercules, CA) with a Dual Color ladder (Bio-Rad, Hercules, CA). In one gel all 18 samples were loaded with 5µl of the ladder added in well 18 alongside the sample. In the other gel sample 14 and 18 were removed and the ladder was loaded into the first and last well with 4µl in the first well and 8µl in the last. The gel was run at 90V for 2 hours, after which the voltage was set to 120V until the lowest band of the ladder ran through at 10 kDa. The running buffer was 10x Tris/Glycine/SDS (Bio-Rad, Hercules, CA) in a 1:100 dilution. Once completed the gels were carefully transferred onto Trans-Blot Turbo Midi PVDF Transfer membranes in transfer cassettes. The cassettes were run on the semidry standard program in a Trans-blot Turbo transfer system (Bio-Rad, Hercules, CA).

After the transfer, the membranes were washed in MeOH for 1 minute, then $H_2O$ for 1 minute, and finally TBS-Tween for 1 minute. The membranes were followingly blocked in 5% skimmed milk in TBS-Tween for 1 hour to prevent non-specific binding of the primary antibodies. If the membranes were examining Flag, they were cut at around 75 kDa so that the Atg13 could be imaged separately from RpS6-P and actin, if the target of the anti-body was GFP the membrane was not cut as to visualize both GFP with the protein and cleaved off on the same membrane. After the blocking and cutting, the membranes were transferred to 50ml Flacon tubes, taking care that the membranes were adhering closely to the sides of the tube with the protein side facing inwards in the tube. They were then left overnight in 3ml of the appropriate primary antibody at 4°C (See table 3.4) in a rotating shaker. The day after the membrane was transferred to a tray and washed 3x5 minutes in TBS-Tween in a tilting shaker with the TBS-T being replaced after each cycle. After the wash the membrane was incubated in secondary antibody appropriate to the primary antibody (See table 3.4). The membrane was then washed again for 4x10 minutes in TBS-Tween before being visualized.

## 3.4.6 Membrane visualization and imaging

To properly visualize the membranes, they were treated with Super ECL PICO and DURA 1:1 (Thermo Fisher Scientific, Waltham, MA) development fluid for 1 minute. PICO is the weaker development fluid and so was always used first if both were to be used. Once treated the liquid was removed and the membranes placed within a plastic sheet which was in turn placed in the imager. The membranes were imaged using a Chemidoc Imaging System (Bio-Rad, Hercules, MA). The imaging settings depended on the antibodies used (see table 3.5). Once visualization was done the membrane was again washed in TBS-Tween for 10 minutes. The membrane was then transferred to a new primary antibody overnight at 4°C. Once all necessary antibodies were visualized the membrane was dried out and wrapped in aluminum foil for permanent storage.

Table 3.5**: Settings for imaging the biochemical assays:** The settings used in the Chemidoc imager to properly visualize bands depending on target.

| Target of primary ABs | PICO [Time(sec)]; Resolution; No. of Images | DURA |
|---|---|---|
| GFP-Atg13 | - | 2-600; 2x2; 10 |
| Atg13-Flag | 2-240; 2x2; 30 | 2-180; 2x2; 20 |
| Ribosomal protein S6 | 2-300; 2x2; 30 | 2-150; 2x2; 20 |
| β-Actin | 2-180; 2x2, 20 | - |

## 3.4.7 Image processing

Image Lab software (Bio-Rad, Hercules, CA) was used to process the images and quantify the bands where relevant. The bands were normalized against actin to show relative expression of Atg13 in different wells. This quantification was done with only two replicates so it could not be used to determine significance. The images were then exported, and they were cropped and rotated using Adobe Photoshop CS6 (Adobe, San Jose, CA). All images were cropped to the same size. The images were then exported in the .tif format.

# Chapter 4

# Results

## 4.1 Cell memory is observed in the autophagic response

Cell memory allows a cell to adjust to changing circumstances by retaining information from previous conditions. Information about previous exposures to factors like temperature[60], salinity[40], and nutrient availability[59] allow the cell to readjust when similar conditions recur. Information is retained by the modification of histones to facilitate the expression of genes that encode proteins useful for adaptation to the previous stimulus. These chromatin modifications are heritable and can be transferred to daughter cells upon budding. Some studies finding memory effects of nutrient availability lasting 12 hours after initial exposure[47]. The aim of this experiment was to observe if this effect is present in the autophagic response. To follow this line of inquiry we used strains of S. Cerevisiae with two genetic reporters, GFP-nG-Atg8 and Pep4-mCherry. Atg8 lines the inside of mature autophagosomes and Pep4 is a protease that localizes to the vacuole. Tracking both markers allowed the observation of the delivery of autophagosomes to the vacuole and thus cellular autophagic activity.  The cells were tracked by high-content live cell imaging at three separate wavelengths, tracking both of the genetic markers and cell surface. A deep learning image analysis approach developed at the Enserink lab then categorized each individual cell as in autophagy or not. The percentage of cells in autophagy was then used as an estimate of the autophagic state of a given strain at a given time. This gave a kinetic of change in the autophagic response over time. A sigmoidal model was fitted to the kinetic using the SICEGAR package in R, which allowed the extraction of its parameters. Specifically, the parameters of interest were the autophagy max, the slope, and the T50. Autophagy max is a measure of the highest level of autophagy reached in the kinetic. The slope is an estimate of the steepness of the kinetic. T50 is the timepoint halfway between the starting autophagy and the maximum level of autophagy reached.

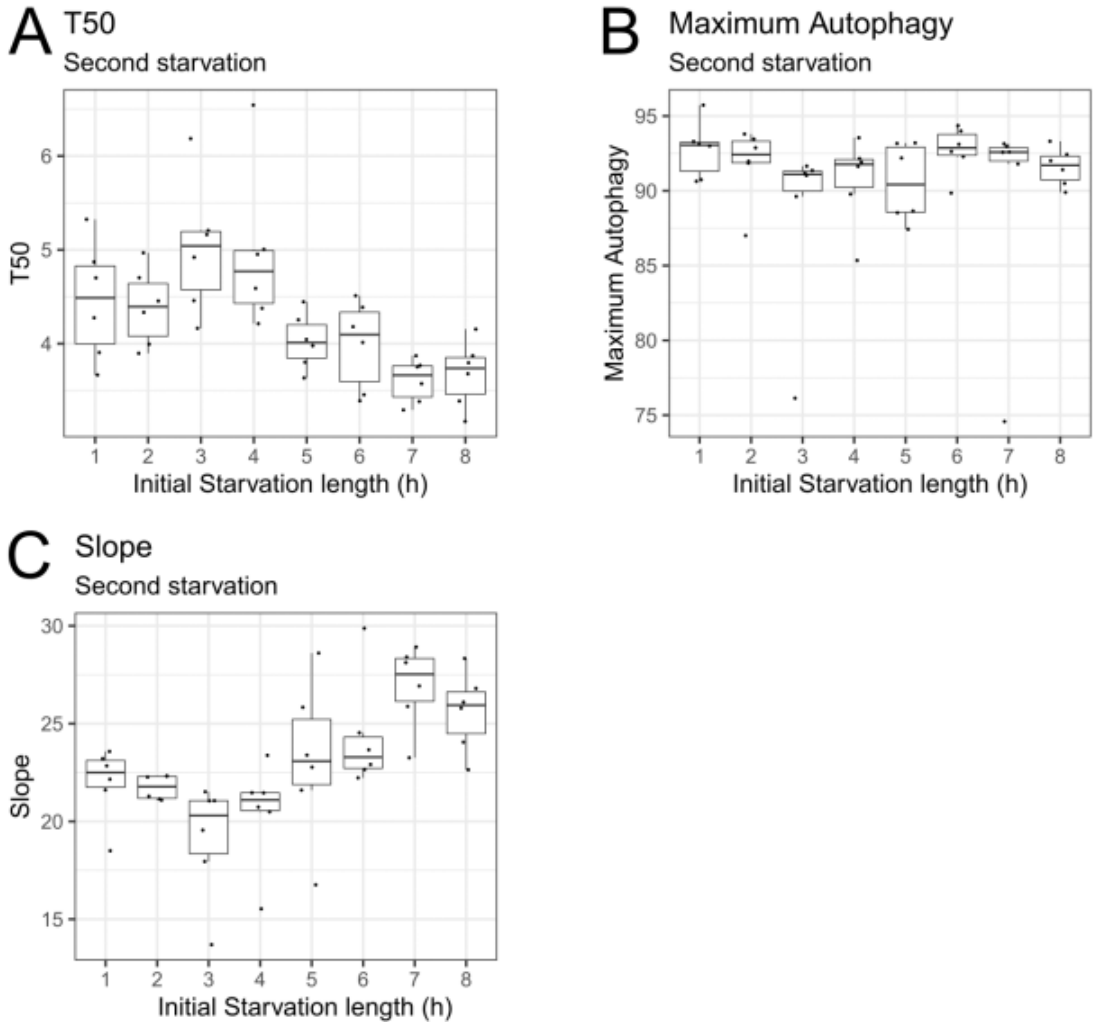


**Figure 4.1: Parameters of autophagy in second starvation with 4-hour replenishment**: Parameters extracted from a sigmoidal model fitted to the second starvation of WT yeast with a replenishment of 4 hours and a second starvation of 12 hours. Each dot representing a specific result. **(A)** T50 values in hours by initial starvation length. **(B)** Maximum percentage of cells in autophagy by initial starvation. **(C)** Slope values of the kinetic by initial autophagy.

To prepare for the experiment, three WT strains of yeast were grown in CSM, a sufficient media, for three cycles to remove any residual memory. They were then imaged through a cycle of starvation, replenishment, and a second starvation period. By varying the length of the initial starvation period and examining the resulting kinetics in the second starvation, we could investigate both the existence of a memory effect and at what initial starvation time it became induced in the cells. Initial starvation times were set between 1 and 8 hours with one hour between each strain, during this time the cells were growing in SD-N. The replenishment phase was set to 4 hours growing in CSM. Finally, a second starvation phase of 12 hours

where the cells were returned to SD-N. We fitted a sigmoidal model to the second starvation to compare the impact of the initial starvation time.

Figure 4.1 displays the parameters extracted from the second starvation by the length of the initial starvation. The T50 increases with a longer initial starvation up to 4 hours of initial starvation, indicating that the cells are taking longer to re-enter autophagy as the starvation gets longer. This indicates a time delay in the onset of memory foundation, the increase in T50 at 3 and 4 hours could also indicate that the cells are struggling to recover after a longer initial starvation and that the memory effect is not strong enough to overcome this. After 5 hours of initial starvation, we see a drop in T50 stabilizing at 7-8 hours (Figure 4.1 A). The early rise in T50 might indicate that there isn't a strong memory effect until 5 hours and when this effect sets in it rescues the T50 and even improves it compared to 1 hour of initial starvation. There are also extreme values in the 3- and 4-hour marks which might exaggerate the effect meaning that the difference between initial starvation times might be smaller than observed. The maximum level of autophagy reached does not seem to follow any discernable pattern (Figure 4.1 B). This implies that there is no memory effect governing the maximum level of autophagy WT cells reach. Notably, the majority of the WT strains operated at max autophagy level of 90% or higher meaning that the cells are operating close to the maximum possible level of autophagy. The slope showed a similar pattern to the T50, with the slope becoming less steep as cells went through a longer initial starvation until 5 hours where the pattern reverses (Figure 4.1 C). This indicates that not just the timing of entry into autophagy improves, but also the efficiency once the process has started.

### 4.1.1 WT yeast shows an autophagic memory effect that persists through at least 7 hours of replenishment

To continue the experiments after having looked at the effect of the initial starvation length, we decided to extend the replenishment period to see if the pattern was still present. The longer replenishment period gives the yeast a chance to recover nutrients and bud daughter cells, it also gives cells a chance to remove any non-memory related residual effect of the initial autophagy. If the effect is present in with a longer replenishment period, it strengthens hypothesis that we are seeing a memory effect transferred from mother to daughter cell. The

new replenishment was set to 7 hours. Based on the previous experiment we decided to use 1 hour, 4 hours, and 8 hours as initial starvation periods. This simplified the experiment while still allowing us to see if the autophagy response followed the same pattern. The results of the longer replenishment are shown in figure 4.2. The effect of initial starvation on the T50 in the second starvation appears similar in 4 and 7 hours of initial starvation (Figure 4.2A). Between 1 hour and 4 hours of initial starvation there is a delay in the onset of autophagy. With an initial starvation of 8 hours the cells enter autophagy earlier than they do for 1 hour, indicating that the memory effect persists. Notably, all the median T50 for all three initial starvation times are lower than the respective medians of 4 hours of replenishment.

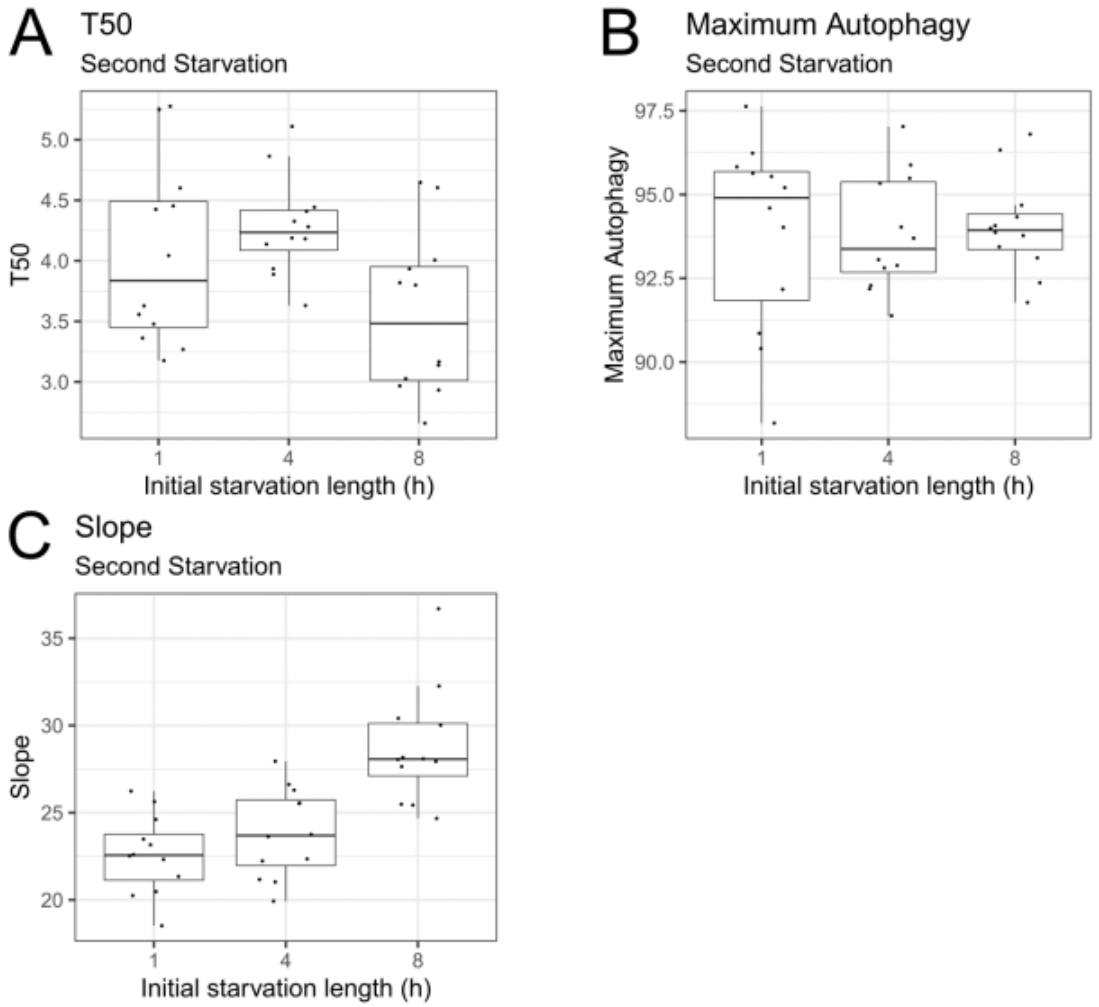


**Figure 4.2: Parameters of autophagy in second starvation with 7-hour replenishment***:* Parameters extracted from a sigmoidal model fitted to the second starvation of WT yeast with a replenishment of 7 hours and a second starvation of 12 hours. Each dot representing a specific result. **(A)** T50 values in hours by initial starvation length. **(B)** Maximum percentage of cells in autophagy by initial starvation. **(C)** Slope values of the kinetic by initial autophagy

As before, the initial starvation does not seem to affect max autophagy reached in the second starvation (Figure 4.2 B). The slope does not display the same pattern as the previous experiment (Figure 4.2 C). In 7 hours of replenishment, a longer initial starvation seems to induce a steeper slope between all timepoints. The decrease in slope seen between 1 and 4 hours of initial starvation in the previous experiment was reversed. A longer replenishment leading to a change in pattern might be because the cells get more time to benefit from the more nutritious media. Cells that have longer to refresh might be more efficient in getting to a maximum autophagy than those in a shorter replenishment. The continued improvement between 4 hours and 8 hours is a strong indicator that the cells are learning.

### 4.1.2 Conclusion to the study of autophagic memory

Two sets of experiments were conducted that both show a clear effect in the second starvation dependent on the length of the initial starvation. The initial experiments showed this effect starting after 5 hours of initial starvation. The second set showed that this effect persists even through 7 hours of replenishment. The improvement indicates that some molecular memory is retained in the cell across periods and is transferred to the next generation. That the effect is present even when the cells go through longer replenishment strengthens this conclusion. This effect is present both in the T50 and the slope indicating that the memory effect causes an earlier onset of autophagy as well as increasing the efficiency with which the cell reaches max autophagy. The T50 and slope largely match except for 4 hours of initial starvation with 7 hours of replenishment. The T50 is a measure of the onset of autophagy and the slope a measure of how quickly the population reaches max autophagy once autophagy has started. The difference we see could indicate that the two effects are not necessarily simultaneous. Seeing as the memory effect has taken effect on the slope and not the T50 it could also indicate that the effect happens as an effect of around 4 hours of initial starvation.

## 4.2 A Genetic screen identified potential regulators of an autophagic memory response

Based on the findings previously described we devised a screen to identify proteins that could potentially regulate the autophagic memory effect that we observed in the previous section.

The mutants used in this screen were selected based on a genome-wide screen done over 5800 single gene-disruption strains executed at the Enserink lab. The genetic reporters and machine learning approach used in the genome-wide screen were the same as used in these experiments, but the methodology was different. The cells in the genome-wide screen were imaged once every hour while growing in SD-N for 7 hours. The parameters from the resulting kinetics were used to create a list of mutants for this experiment. The mutants that were selected displayed a disruption in autophagy, but still had sigmoidal autophagy kinetics. This list was further narrowed down using gene ontology terms relevant to the regulation of gene expression or cellular mechanisms. Specifically, the terms used were signaling, transcription, translation, mRNA processing, and chromatin remodeling. This resulted in a list of 67 mutants (see table 3.1), grown on 4 separate 96-well plates. Two wells didn't show growth, namely *ssn2Δ* and *npl3Δ* and so weren't used further. Each plate had two WT strains that were used in the previous experiments in addition to one strain of *atg1Δ*, functioning as a negative control. To attempt to capture the kinetics we had previously observed, we chose 1 hour, 4 hours, and 8 hours of initial starvation times during which the cells were exposed to SD-N. The replenishment period was 4 hours in CSM. The second starvation period was 12 hours in SD-N.

The predictions were made, and sigmoidal models were fitted to all strains in the experiment and the parameters were extracted. The parameters were used to construct cleaned curves of all strains (Figure 4.3 and figure 4.4). The most obvious observation is that there is no autophagy response in the *atg1Δ* controls, indicating that the autophagy observed in the remaining wells is correct. *Atg14Δ* (Figure 4.4A) also showed no autophagy response regardless of initial starvation times, and so was not explored further. A cursory overview shows a great deal of variation in the autophagy response of the mutants, but a general similarity in the WT strains. To ensure a memory effect was present in the WT strains we started by examining them a little closer (Figure 4.5). T50 values decreased as the cells went through longer periods of initial starvation (Figure 4.5 A). Previously we had observed an increase in T50 at 4 hours of initial starvation that dropped as the initial starvation become longer. The change in the observed pattern indicates that the effect in that timepoint is somewhat less reliable. Because of an irregularity in the slope at 4 hours we previously indicated that the effect of memory might begin closer to 4 hours of initial starvation, which might explain the change we see in the T50 parameters.

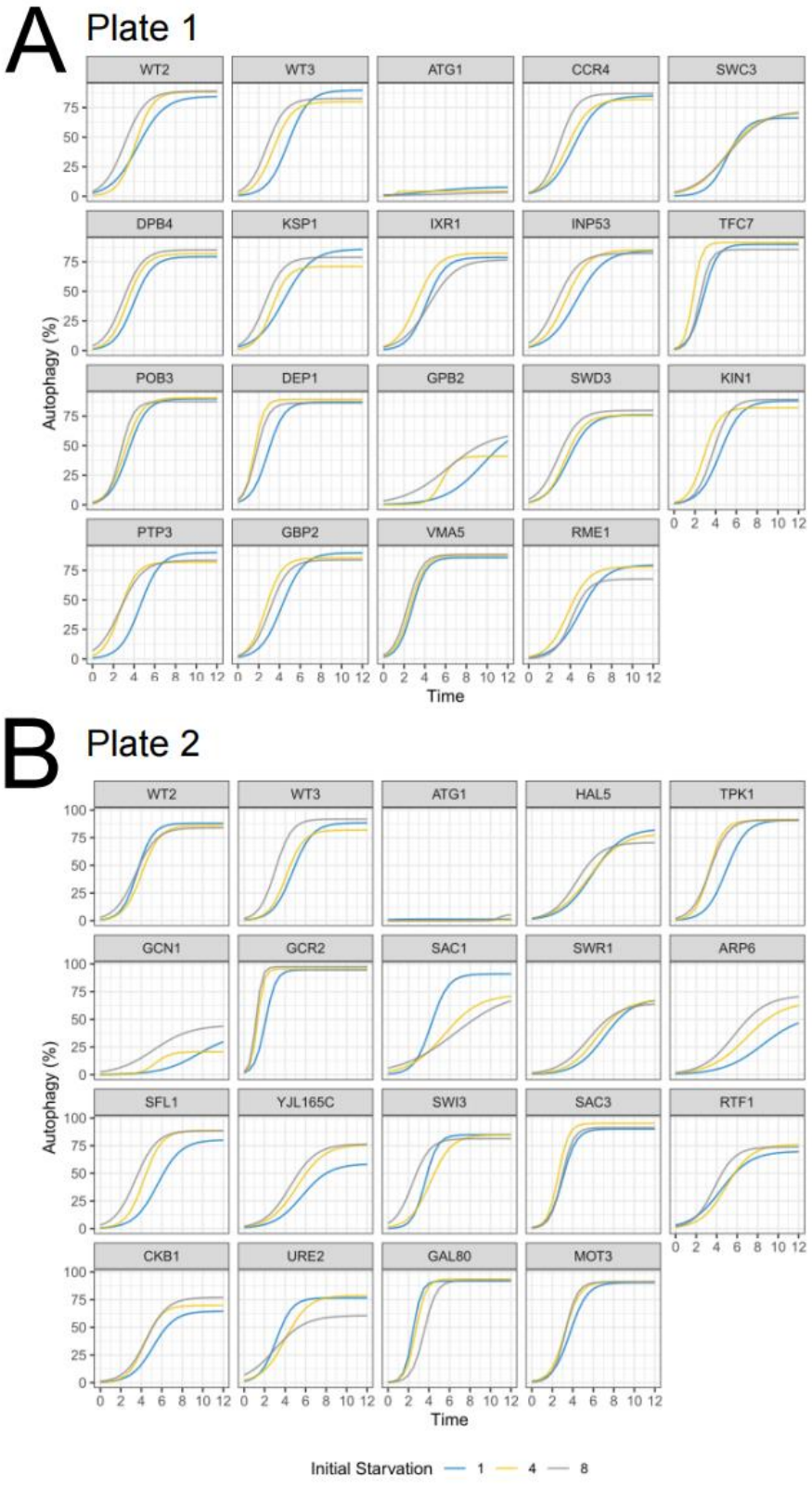


**Figure 4.3: Cleaned curves of the second starvation of the first two plates in the screening.** The effect of varying initial starvation on the second starvation of mutants in the screen. Curves were reconstructed from parameters extracted from the sigmoidal model fitted to the second starvation of all strains in the genetic screening. **(A)** Strains from the first plate. **(B)** Strains from the second plate.

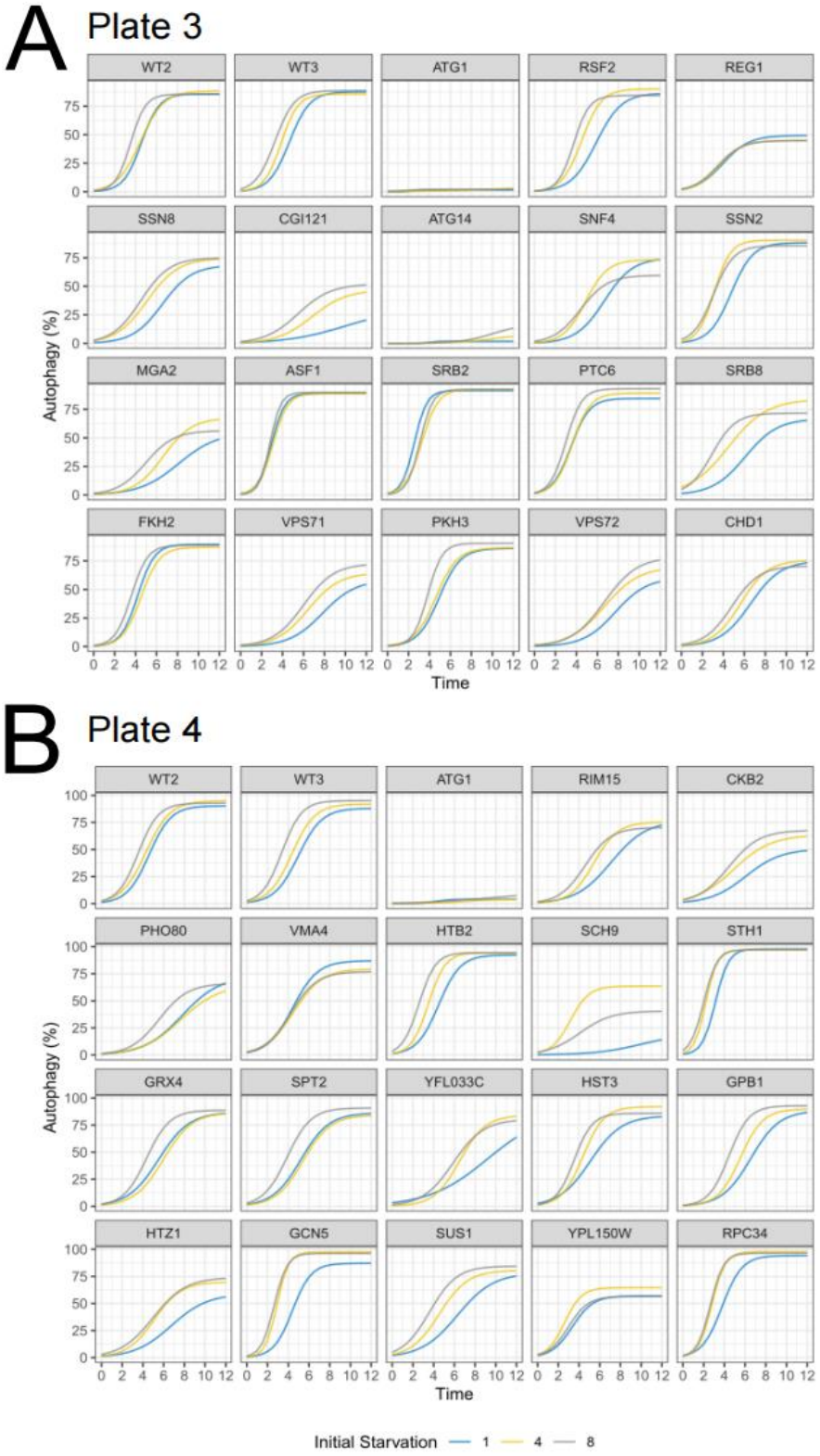


**Figure 4.4: Cleaned curves of the second starvation of the second two plates in the screening.** The effect of varying initial starvation on the second starvation of mutants in the screen. Curves were reconstructed from parameters extracted from the sigmoidal model fitted to the second starvation of all strains in the genetic screening. **(A)** Strains from the third plate. **(B)** Strains from the fourth plate.

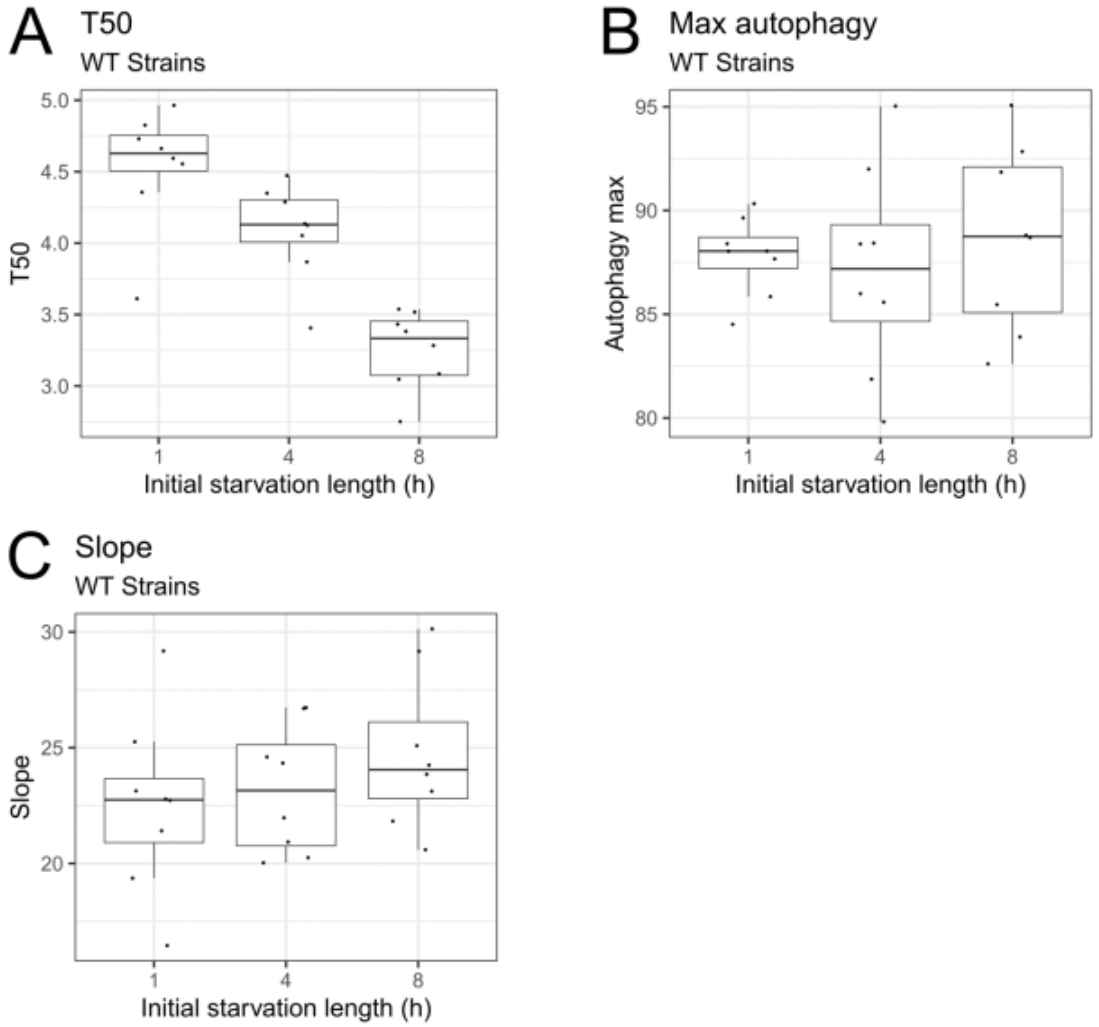


**Figure 4.5: Parameters of the WT strains in the screen.** The parameters of the second starvation of 8 WT strains imaged in the genetic screen. Each strain went through 4 hours of replenishment and 12 hours of second starvation. **(A)** T50 values by initial starvation in hours. **(B)** Percentage values for maximum autophagy by initial starvation. **(C)** An estimation of the increase in autophagy per hour by initial starvation.

Regardless, there is a clear difference observed in the T50 of the WT strains indicating a memory effect. The maximum autophagy displays the same pattern as before, with no difference based on previous starvation times observed in WT strains (Figure 4.5 B). There does seem to be improvement in the slope, but the median values are very close together making it harder to draw conclusions from it (Figure 4.4 C). The weak pattern observed in the slope does match the pattern seen in the results of 7 hours of replenishment in figure 4.2, specifically an increase in the slope as initial starvation gets longer.

### 4.2.1 Differences in WT and in mutant parameters

To compare the differences in response in the mutants, we extracted the T50, slope and maximum autophagy from the growth kinetics from all the strains. The differences in the three parameters based on initial starvation times for each individual strain were calculated. Individual differences in T50 (Figure 4.5) and autophagy max (figure 4.6) were charted in waterfall plots.

The difference in each parameter for each mutant was ordered going from smallest to greatest difference with bars indicating standard error to find mutants of potential interest. The slope was also extracted and compared but these differences have a much wider error and it was harder to draw conclusions from them (Figure S6, S7, and S8). Figure 4.6 shows the differences in T50 based on the initial starvation periods by mutant. Firstly, the strains do not seem to cluster by plate meaning we aren't seeing an obvious batch effect. In Figure 4.6A there difference in WT differences spans between 0.2 of difference to 2.1 hours. The lower number seems to be caused by WT2 in Figure 4.3B overperforming at 1 hour of initial starvation. Most strains fall inside the span, but those mutants that exceed it are of interest as it implies that the mutant learns or retains memory more effectively than WT strains. Strains that fall below 0 are also interesting as they do not display the learning effect observed in WTs. A difference far below 0 implies that the mutation inhibits the onset of autophagy in the second starvation. The difference between 4 hours and 8 hours should be smaller based on Figure 4.4A and this is observed in Figure 4.5B with a span of 0.6 hours to 1.1 hours in difference. Again, any strain with a difference below 0 is interesting. Strains improving the re-activation of autophagy could imply a function as a negative regulator of autophagy. Finally, figure 4.5 C shows the differences in T50 between 1 and 4 hours. The span in difference in WTs in Figure 4.5 goes between -0.6 and 1.4, based on figure 4.4A there shouldn't be that great a difference in T50, so the span makes sense.

So far, every experiment has verified that WT yeast does not show any pattern in its maximum autophagy response based on initial starvation times. Looking at figure 4.7, it does appear that this still holds true, with the differences in WT strains all grouping around 0. On the other hand, some mutant strains show a large difference in maximum autophagy across different initial starvation periods. There is no grouping in the autophagy max meaning that there is no batch effect. When WT cells have been put into autophagy in these experiments, they have all reached a level of around 85-95% of cells in a given well being in autophagy

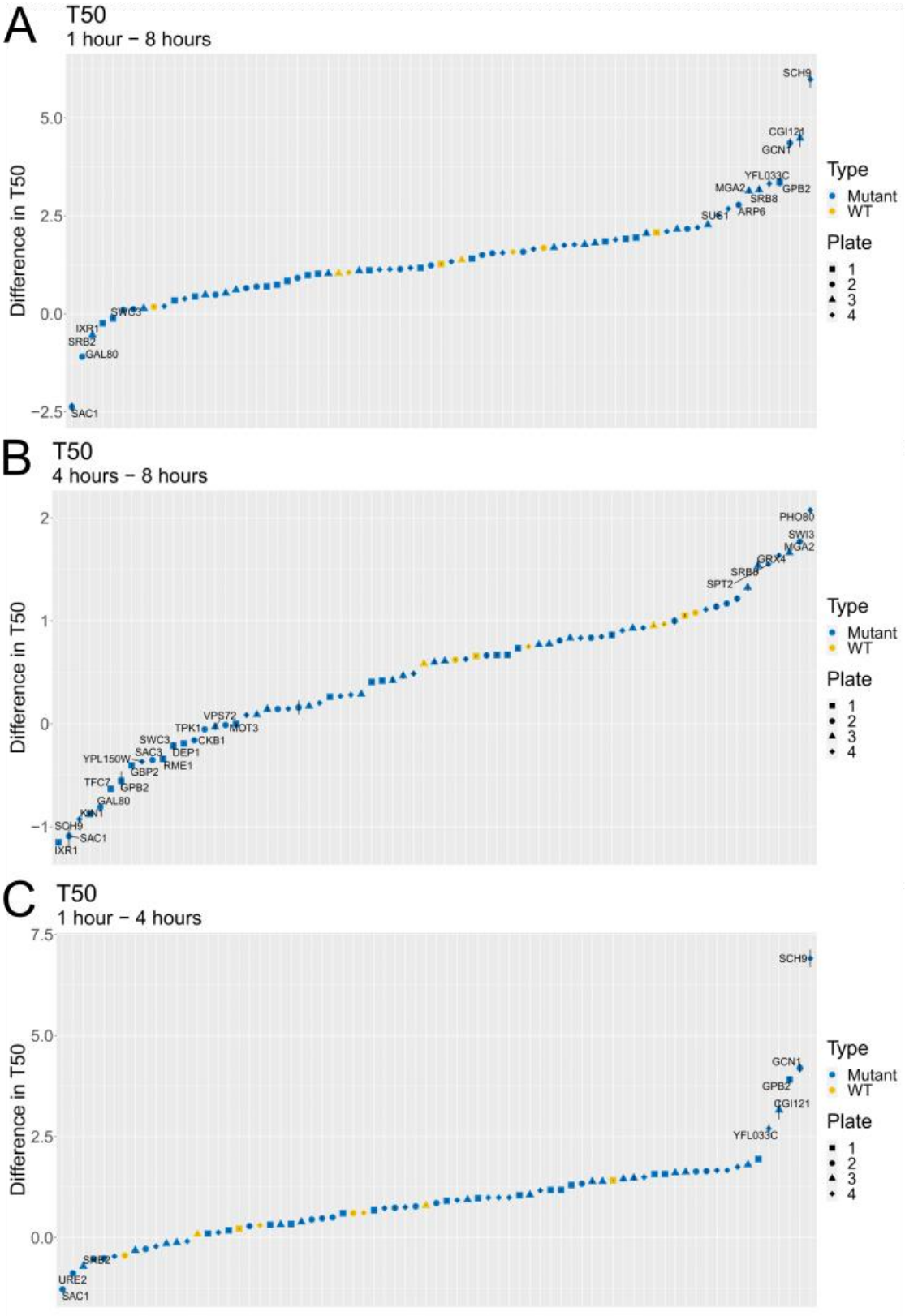


**Figure 4.6: Differences in T50 among mutants and WT strains in the genetic screen.** Differences in T50 parameter extracted from the second starvation of a genetic screen. Plotted in ascending order with the shape indicating the batch and color representing mutant or WT status. (A) Differences found between 1 and 8 hours of initial starvation. (B) Differences between 4 and 8 hours of initial starvation. (C) Differences between 1 and 4 hours of initial starvation.

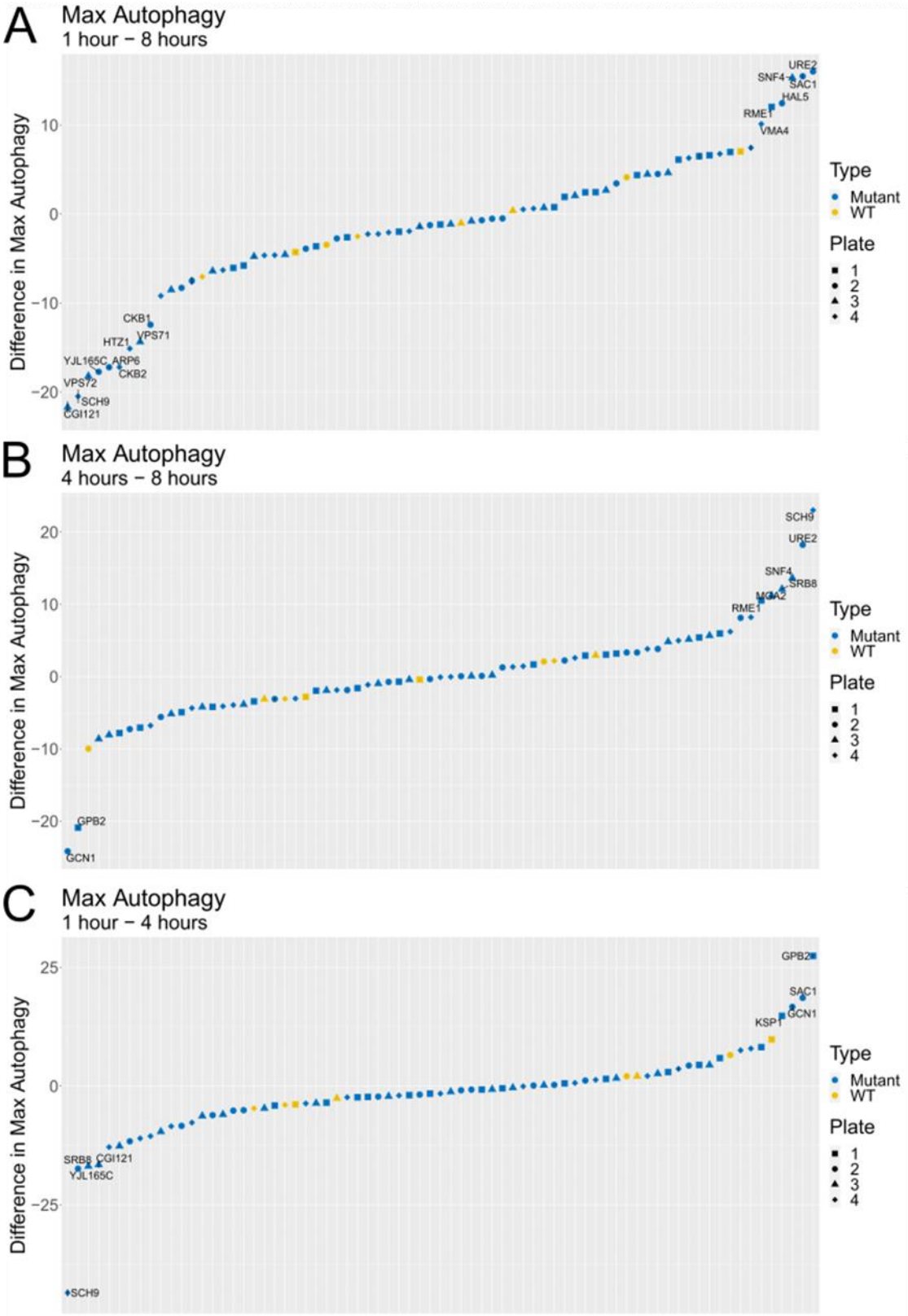


**Figure 4.7: Differences in maximum autophagy among mutants and WT strains in the genetic screen.** Differences in Autophagy max parameter extracted from the second starvation of a genetic screen. Plotted in ascending order with the shape indicating the batch and color representing mutant or WT status. (A) Differences found between 1 and 8 hours of initial starvation. (B) Differences between 4 and 8 hours of initial starvation. (C) Differences between 1 and 4 hours of initial starvation.

(Figure 4.1B, 4.2B, and 4.5B). Many of the mutants do not reach this high a level of autophagy and seem to show distinct memory effects. It could be that these mutants display an effect that is masked in WT strains because they all reliably reach the highest max autophagy level. A reduction in autophagy max outside the scope of the WT indicates some difficulty in the full re-activation of the autophagy response. A reactivation outside the ranges of the WT cells indicate that the mutation is allowing greater activation in the cells. As noted previously, all mutants with a notable difference also have some disruption in the max autophagy they can reach. In figure 4.7A we see difference in autophagy max in WTs on a spectrum ranging from -7.04 to +7.03. The spectrum of WT differences in Figure 4.7B ranges from -9.97 to 2.95 and in figure 4.7C it ranges from -4.69 to 9.83. There is not expected to be a pattern to the differences in the WT and so those that fell outside of the highest and lowest measured differences, -9.97 and 9.83, were noted.

## 4.2.2 Grouping the differences gave a list of mutants of interest

We used the superheat function in R to find groupings of mutants in a heatmap (Figure 4.7). While the difference in slope had a great deal of error it was still used to find potential groups in the experiment. As the intent of this experiment is to find potential mutants showing a memory effect, we decided to use the information from the differences in slope while being aware of the uncertainty in it. The grouping of columns shows that the 1h-8h and 1h-4h differences within each parameter are the most closely grouped. The 4h-8h differences do not follow the same pattern. Of the mutants *sch9Δ* shows the most divergent results, grouping with no other mutant. Sch9 is one of the main targets of TORC1 and is involved in mediating many of the intracellular effects of TORC1[68]. Looking at Figure 4.4 B we can see that it had a very weak kinetic at 4 hours of initial starvation and a wide divergence between 1 hour and 8 hours of initial starvation. Figures 4.6 and 4.7 show that *sch9Δ* has extreme values in almost all waterfall plots. The lack of grouping with any other mutant is likely because of the weak autophagy response after 4 hours of initial starvation, meaning the experiment should be repeated, but *sch9Δ* might be interesting to look at. Outside of SCH9 some other clusters also remain fairly removed from the WT strains. *srb8Δ, mga2Δ, hst3Δ, rsf2Δ, CGI121Δ*, and *arp6Δ* all show more improvement in the T50 than WT strains. Some, but not all show a

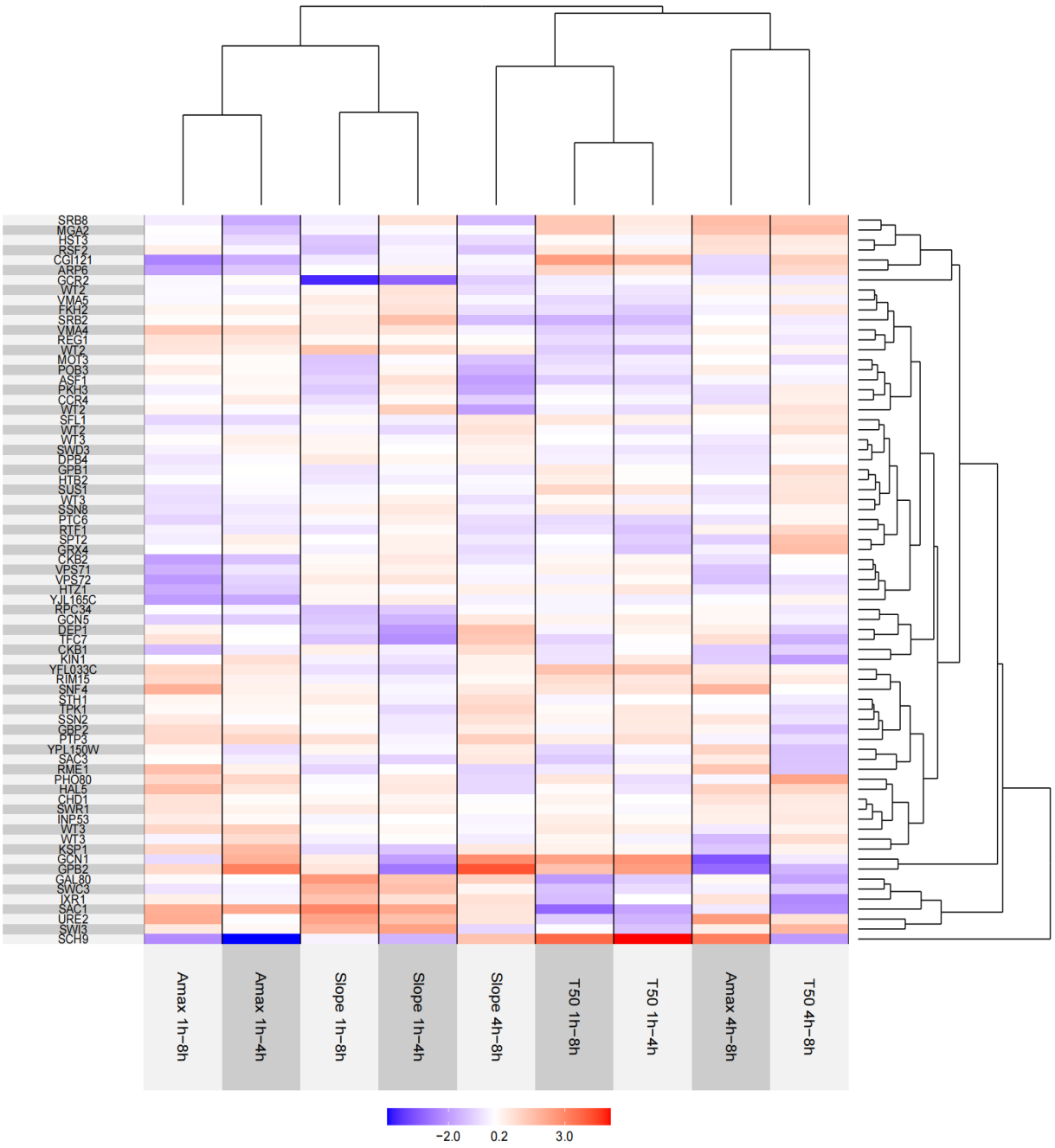


**Figure 4.8: Heatmap showing the grouping of mutant strains based on the differences in parameters based on initial starvation.** Mutants grouped by differences in parameters maximum autophagy (Amax), T50, and Slope in a heatmap made with Superheat. The values are normalized (mean=0, standard deviation=1) using the scale=TRUE function. The Dendrograms show closeness of relation in the parameter differences and in the mutants.

decrease in maximum autophagy with longer initial starvation periods. *Gpb2Δ* and *gcn1Δ* also cluster together, looking at figure 4.3A & B it is clear both mutants display a greatly reduced maximum autophagy around 50%. They also show a strong improvement in T50 when exposed to longer initial starvation periods. Finally, *gal80Δ, swc3Δ, ixr1Δ, sac1Δ, ure2Δ, and swi3Δ* cluster together. They all show an increase in T50 and a reduction in slope when the initial starvation period is longer. There is no specific pattern in the maximum level of autophagy these strains reach.

### 4.2.3 Several mutants show direct links to established mechanisms of memory

Some of the mutants that do not group with WT strains are interesting in regard to memory, several mutants of interest have histone modifying or chromatin remodeling effects which is a common underlying mechanism of memory. Both *swc3Δ* and *swi3Δ* show either no improvement in T50 or a negative difference which shows an inhibition in the memory effect. The mutants are both part of the SWI/SNF complex, a chromatin remodeling complex that is crucial in the formation of GAL gene memories[58]. The activity of this complex specifically displaces the canonical H2A and H2B histones from chromatin in an ATP-dependent manner. The fact that these mutants show no memory effect fits very well with the current understanding of the SWI/SNF complex. *arp6Δ* shows a memory effect that improves beyond that of WT strains in both the autophagy maximum and the T50. Arp6 is part of the SWR1 complex, which interestingly replaces canonical H2A with H2A.Z. Specifically Arp6 is necessary for the binding of the complex to the substrate H2A and the proper function of the complex[69]. The improvement in the memory that is seen in the *arp6Δ* mutant indicates that the form of chromatin remodeling performed by Arp6 might be negatively regulating memory effects. Histone modifiers are also potentially important for memory and the *hst3Δ* mutant shows a distinct improvement in its memory effect as the T50 decreases and autophagy max increases with prolonged initial starvation. Hst3 is a sirtuin histone deacetylase involved in the repression of gene expression, the protein is kept stable by continued TORC1 activity[70] and is believed to be necessary for cell growth and the cellular stress response. That the mutant shows an improved memory response might indicate that Hst3 also has a role in the downregulation of the memory response. Gal80 is a transcriptional repressor of the GAL gene cluster when the cell signals the presence of glucose in its environment. The GAL gene

cluster has an established memory effect in repeated exposure to galactose[47]. That *gal80Δ* shows an increasing T50 based longer initial starvation periods seems to indicate that Gal80 plays a role in upregulating memory in the autophagy response.

The *srb8Δ* mutant (Figure 4.4 A) shows an improvement in memory as expressed through T50 and autophagy max when going through longer initial starvation periods. Srb8 is a part of the RNA Pol II mediator complex, specifically in a subunit which is seemingly associated with transcriptional repression[71]. As noted previously, one mechanism of memory is defined by the binding of a poised version of RNAPII to the promotor of the gene of interest. The phenotype of this mutant could imply that mediation of RNAPII binding could influence the memory effect in yeast.

### 4.2.4 Mutants with direct metabolic roles are also worth examining

Some mutants are directly linked to autophagy or nitrogen metabolism, which makes them potential mediators of a memory effect as well as potential regulators of memory. Gpb2 is a regulator of protein kinase A (PKA), capable of inhibiting its three catalytic subunits independently of the cAMP levels in the cell[72]. The catalytic subunits of PKA phosphorylate Atg13 and Atg1 to inhibit autophagy. The *gpb2Δ* mutant shows a distinctly different phenotype at 4 hours of initial starvation (Figure 4.3A) explaining why it is grouped with only one other mutant. This phenotype isn't disqualifying and the difference in T50 between the 1 hour and 8 hours of initial starvation is also an extreme value, with a reduced T50 value when exposed to longer initial starvation periods (Figure 4.6A). Another mutant directly linked to nitrogen metabolism is *sac1Δ*, which shows a much more efficient second starvation when the initial starvation period is only 1 hour. The Sac1 is a phosphoinositide phosphatase that acts on several phosphatidylinositol molecules, importantly on phosphatidylinositol 4-phosphate (PtdIns4P). PtdIns4P are found in autophagosomes and the phosphatase activity of Sac1 on these lipids seems to be essential for vacuolar fusion[73]. Decreased Sac1 activity in the cell leads to abnormal incorporation of PtdIns4P in Atg9 vesicles. The change in the lipid composition of the vesicles leads to SNARE proteins being unable to integrate the autophagosome into the vacuole/lysosome[74]. Mammalian cells without Sac1 are incapable of entering autophagy at all. Neither Sac1 nor Gpb2 appear to

have an intrinsic ability to modify chromatin or confer memory themselves, but both are interesting as potential mediators of a memory response. Ure2 is a regulator of the localization of transcription factor Gln3 and Gat1[75], which control the expression of genes related to nitrogen catabolite repression. Nitrogen catabolite repression is a regulatory mechanism that prevents the expression of proteins that utilize poor nitrogen sources when higher quality nitrogen sources are available. When quality nitrogen sources are abundant in the cell Ure2 binds Gln3 to prevent its localization to the nucleus and thus prevents TF activity from Gln3. Ure2 activity is controlled by TORC1. Notably, Ure2 can also form the prion [URE3][76], which could theoretically be a mechanism that confers memory on the cell.

## 4.3 Biological assays of autophagic memory

The experiments so far have given grounds for the presence of a memory effect and a list of potential mutants of interest. The next step in the experiments was to relate these results to an underlying biological process expressing the memory effect that we have observed so far. The onset of autophagy is inhibited by the direct hyperphosphorylation of Atg13 by TORC1 which prevents the formation of a Atg1 complex. So far, we have seen that memory leads to an earlier and more efficient onset of autophagy. One potential underlying process could be a faster and more efficient dephosphorylation of Atg13 in response to starvation. To assess this and to examine the phosphorylation of Atg13 through the autophagic response, we used a strain containing a Atg13-GFP plasmid. Because Atg13 has multiple potential phosphorylation states it visualizes as a smear in the membrane when the protein is not dephosphorylated, whereas when it is dephosphorylated, it will show as one distinct band on the membrane. The strain was grown and sampled through a cycle of starvation, replenishment, and second starvation. This line of inquiry was performed through three experiments varying the initial starvation and replenishment (Figure 4.8). Phosphorylation of Rps6 is promoted by TORC1 and so was used to monitor TORC1 activity[77] as a way of examining autophagy. Actin was used a loading control. Free GFP is the cleavage product of Atg13-GFP, Atg13 is broken down quickly, but GFP takes longer for the cell to break down. The presence of free GFP in the assay suggests that the cell is breaking down Atg13 proteins. Figure 4.8 A shows WT yeast through a cycle of 8 hours of initial starvation, 4 hours of replenishment, and 12 hours of second starvation. In t0, the cells are in a nutrient rich

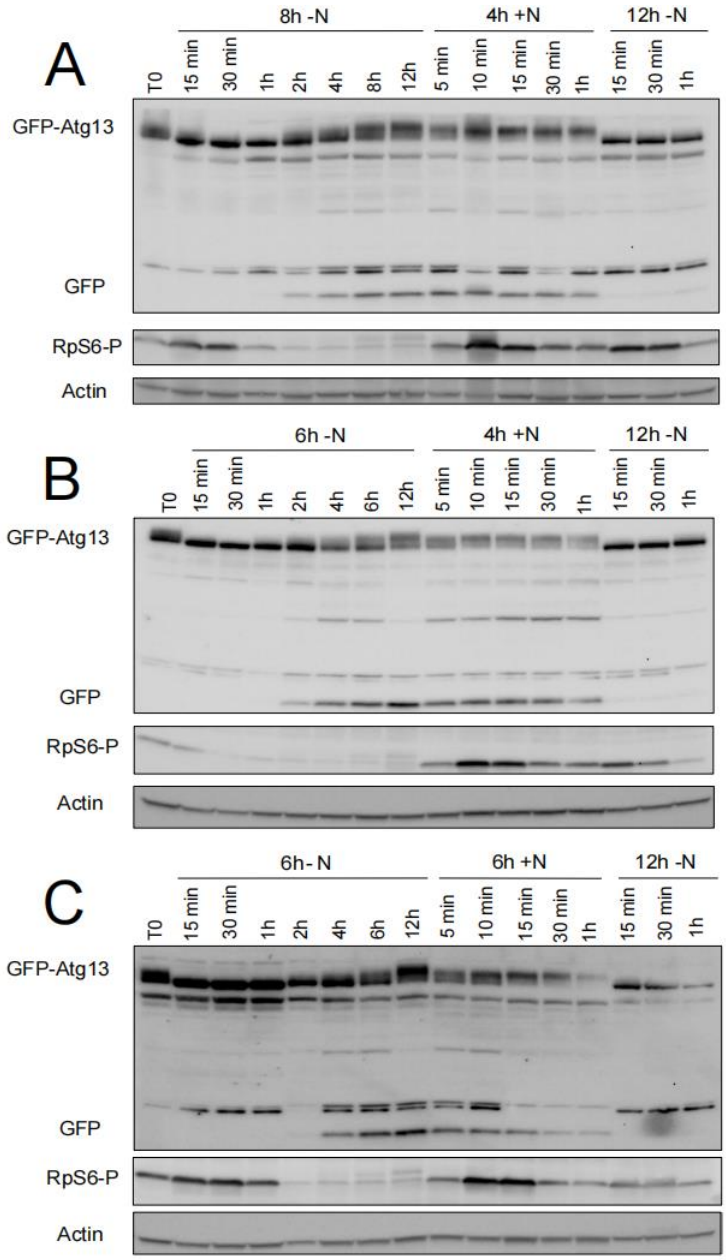


**Figure 4.9: Assays monitoring phosphorylation of Atg13 in WT yeast**. A WT strain containing a GFP-Atg13 plasmid was grown in a cycle of starvation, replenishment, and second starvation. Each phase was grown as a separate batch with overlapping timeframes. All three assays were treated with antibodies mapping GFP, RpS6 phosphorylation, and Actin and had different timeframes. **(A)** The experiment had 8 hours of initial starvation, 4 hours of replenishment, 12 hours of second starvation. **(B)** The experiment had 6 hours of initial starvation, 4 hours of replenishment, 12 hours of second starvation. **(C)** The experiment had 6 hours of initial starvation, 6 hours of replenishment, 12 hours of second starvation.

environment and so Atg13 remains dephosphorylated. Atg13 does undergo a rapid dephosphorylation at the onset of nitrogen starvation and stays dephosphorylated for the first hour of starvation before beginning to rephosphorylate around 2 hours. The smear indicating rephosphorylation becomes notably more spread in the 4-hour mark and is fully spread by the 8-hour mark. This process is not matched by phosphorylation of RpS6 meaning we don't see a TORC1 reactivation. 2 hours is also the timepoint where free GFP starts becoming visible in the blot, indicating that breakdown of GTP-Atg13 has begun. Breakdown of GFP-Atg13 continues for the rest of the starvation period and into the replenishment. Once in

replenishment the phosphorylation state of Atg13 remains the same, but as expected there is increased RpS6-P indicating increasing TORC1 activity.

As the cells enter the second starvation period, we see a slightly sharper dephosphorylation at 15 minutes of initial starvation. Sharper dephosphorylation implies a more rapid re-activation of the autophagic machinery in the cells. Notably, the free GFP is immediately gone indicating that the cell is no longer breaking down Atg13.To further examine the dephosphorylation speed in the second starvation, we changed the timing of the initial starvation to 6 hours to see if the shorter initial starvation time would kill the effect (Figure 4.8B). The improvement in the second starvation seems to be present in this experiment as well. Interestingly, at the 6-hour mark of the initial starvation there is a clearer dephosphorylated band than seen in 8 hours of initial starvation indicating that full

rephosphorylation of Atg13 happens somewhere between 6-8 hours of nitrogen starvation. To see if there was any change in the pattern, we extended the replenishment time (Figure 4.8 C). The pattern did seem to follow the same general trend of the previous experiment, with the dephosphorylation in the second starvation seemingly being more efficient than in the first, though this effect is harder to evaluate because of a technical error in the blot. All three assays seemingly show a weak improvement in the dephosphorylation of Atg13. This could be an expression of memory, but it would require further experimentation and more sensitive assays to draw a clear conclusion.

### 4.3.1 Transcription assays of Atg13 show a clear memory effect

The previous set of experiments looked at the signaling response in autophagic memory, but another possible expression of memory could be the relative expression of Atg13 proteins. One form in which cell memory is expressed through more rapid transcriptional re-activation because RNAPII is already bound and poised to the gene of interest. To examine the possibility of memory being expressed through rapid transcription, we grew a WT strain containing Atg13-5x-FLAG through the same cycles of initial starvation, replenishment, and second starvation (Figure 4.9). In addition to the blot the results were quantified to examine the scope of the difference in expression of Atg13. Looking at the quantifications there is an elevated level of expressed Atg13 in the second starvation phase (Figure 4.9A). This effect is weaker when the starvation time is longer but is still present (Figure 4.9B). Samples were

collected for 4 hours of replenishment and 12 hours of second starvation as well, but unlike the rest of the timepoints they were only blotted once and were therefore not quantified. Importantly, the clearance of Atg13 is not the same in the two replenishments with 4 hours of

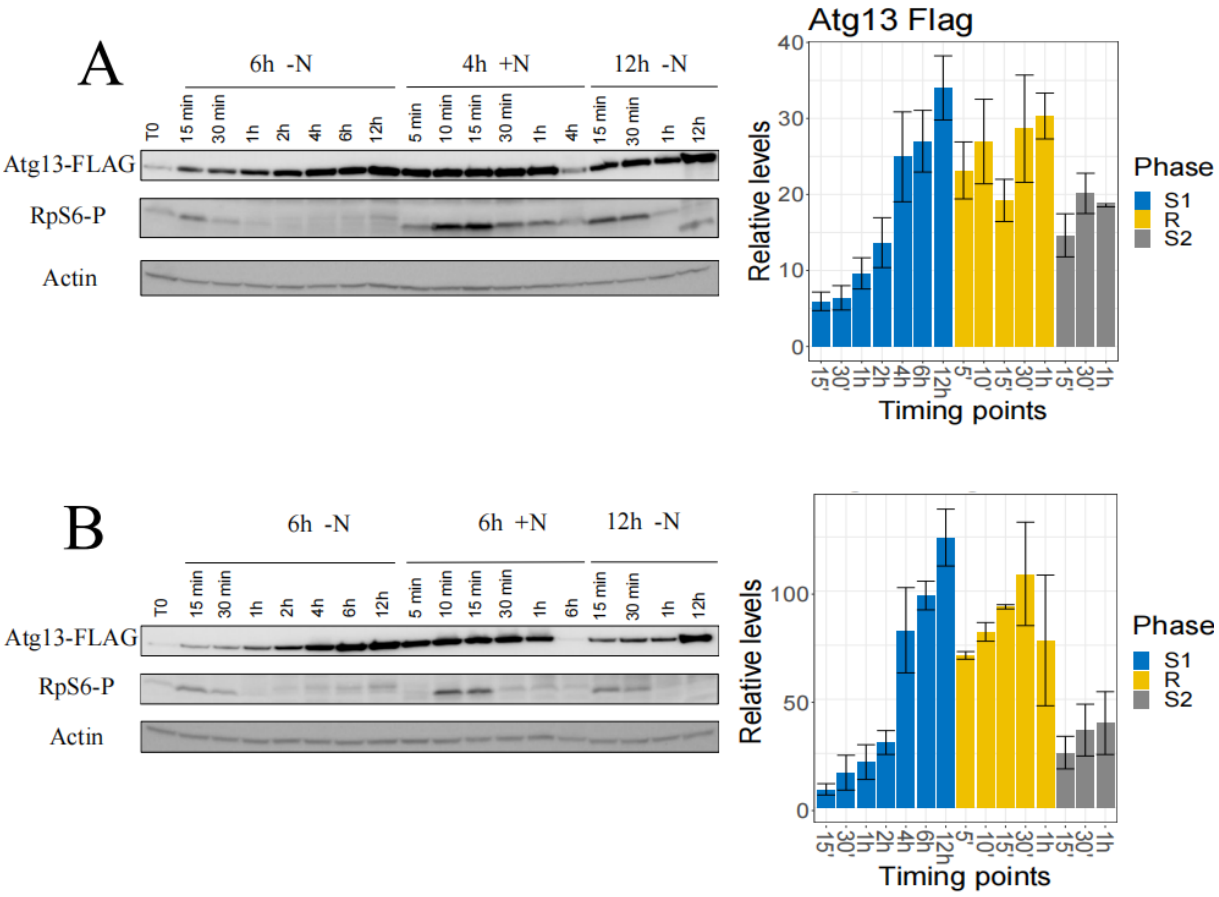


**Figure 4.10: Assays monitoring the expression of Atg13 in WT yeast with quantifications**. A WT strain containing a plasmid with Atg13-FLAG grown through a cycle of starvation, replenishment, and second starvation. Each experiment had a separate timeframe. The related quantifications were drawn from two replicates. **(A)** Timeframe of 6 hours of starvation, 4 hours of replenishment, 12 hours of second starvation. **(B)** Timeframe of 6 hours of starvation, 4 hours of replenishment, 12 hours of second starvation.

replenishment showing a much more visible Atg13 band remaining in the blot. The Atg13 band is fully cleared after 6 hours of replenishment. It is possible that the difference in Atg13 levels seen between the two blots might be a consequence of residual Atg13 in Figure 4.10A. However, both blots show heightened levels of expression of Atg13 after entry into the second starvation indicating cell memory. Looking at the levels through the experiment, it is also clear that there is a notable increase in the expression of Atg13 between the 2-hour mark

and the 4-hour mark in both blots. This corresponds with the onset of rephosphorylation of Atg13 as seen in Figure 4.9. The similar timing might indicate a link between these two processes.

# Chapter 5

# Discussion

## 5.1 The autophagic response in yeast cells is modified by a memory mechanism

The focus of this thesis has been the expression of memory in the autophagic response in *S. cerevisiae*. The expression of memory is an adaptive process allowing for the cell to change its phenotype in response to changing environmental circumstances. While the specific focus on memory in the autophagic response is new, the presence of a memory effect in response to changing nutrient availability in *S. cerevisiae* is not. Much work has been done to properly elucidate the memory mechanisms in the GAL gene cluster[47] and in the expression of INO1[46]. Still there remain unanswered questions within these mechanisms about the formation and maintenance of cell memory. Importantly, there are also differences between the two memory systems, indicating that cell memory can take different forms depending on the genes being expressed. GAL gene expression is highly dependent on Gal1, a cytosolic protein that is sufficient to trigger a memory response in the cell[59]. No such protein has been found in the memory mechanisms of INO1. The two models also rely on different interactions with the nuclear pore complex where GAL gene expression appears to be dependent on an intragenic loop interacting with a nuclear pore protein[46]. As noted in the introduction, the process of memory does appear to have some central common mechanisms.

The first step in this project was to prove the presence of a memory effect in the autophagic response in *S. cerevisiae* cells. Growing cells through cycles of starvation and replenishment showed that re-activation of the autophagy response is sensitive to changing periods of initial starvation. As we didn't have a control strain that only went through one starvation period, we cannot say for certain what the effect of initial starvation is compared to a strain that didn't go through any initial starvation. That having been said, there is good indication of a memory effect in the effect we see in the second starvation based on changes to initial starvation times.

From the results of the biological assays, we also see that the first hour of initial and second starvation have notable differences. The second starvation showed a sharper dephosphorylation of Atg13(Figure 4.9) and a more rapid expression of Atg13 (Figure 4.10). All of this provides strong evidence of a memory effect in the autophagy response of *S. cerevisiae*.

## 5.2 The memory effect seems to require prolonged exposure to nitrogen starvation.

It would not be adaptive for cells to retain strong re-activation responses to stimulus that is not likely to recur. One of the questions we sought to answer was how long lasting the effect of nitrogen starvation had to be for the cell to respond with a memory effect upon reintroduction to the stimulus. In the study of autophagic memory we saw that cells in an initial starvation of 5 or more hours showed improved T50 and slope in the entry into autophagy (Figure 4.1 A& C, Figure 4.2 A& C). The WT strains in the screening showed an improvement in 4 hours not observed in the previous experiments (Figure 4.5 A). We theorized previously that the change in the T50 in the second starvation happened closer to 4 hours of initial starvation because we saw a change in the pattern of the slope in figure 4.2 C. Simultaneously, we saw that the rephosphorylation of Atg13 and the Atg13 both became more notable in the 4-hour mark of the assay (Figure 4.9 and 4.10). The rephosphorylation of Atg13 indicates a decreased entry into autophagy as the cell goes deeper into nitrogen starvation. Meanwhile an increased expression of Atg13 creates more proteins that can be dephosphorylated to initiate autophagy. Two seemingly opposite responses to starvation.

It is possible that the change in memory effect around the 4-hour timepoint is related to increased expression levels of proteins which could function as cytosolic components similarly to the function of Gal1 in the memory response seen in the GAL gene cluster[47]. Some forms of proteins, when overexposed, will show memory effects several generations after first exposure[63]. While we cannot causally determine the effect in these experiments, increased levels of Atg13 in the cell during replenishment also seemed to correlate with faster re-activation upon re-induction to starvation in as seen in Figure 4.10A & B. Importantly, there is no known cytosolic component that drives autophagy re-induction in *S. cerevisiae* cells and there is not enough evidence to conclude that one exists based on these results. Even

if it is not the expression of a cytosolic factor, the changes in expression that the cell undergoes at the 4-hour timepoint are still notable for their similarity to the time needed to trigger a memory effect upon exposure to nitrogen starvation.

## 5.3 The memory response appears to involve chromatin remodeling

One common aspect of both GAL memory and INO1 memory is the necessity of heritable forms of chromatin remodeling. This happens through the re-localization of the gene to the cell nucleus where it interacts nuclear pore proteins to stabilize that localization through several generations[46]. Once localized the nearby histones are modified to facilitate memory a memory response in the cell. The mutant screen showed that *swc3Δ, swi3Δ, and arp6Δ* all showed notably different phenotypes from WT yeast in the experiment. All three mutants are involved in the remodeling of chromatin, *swc3Δ* and *swi3Δ* are both part of the SWI/SNF complex which is responsible for the displacement of H2A and H2B histones in around the binding site of the gene of interest. This effect is seemingly essential for GAL gene memory in the cell[58]. These two mutants showed disruption in the autophagic memory effect that had previously been observed in the T50 of WT cells. This is a strong indicator that SWI/SNF dependent chromatin remodeling takes place in the autophagic response. The *arp6Δ* mutant showed an improvement in its memory response across both T50 and maximum autophagy. Arp6 is part of the SWR1 complex which exchanges H2A histones with H2A.Z, a histone variant found to be important in most forms of memory[56]. Notably, however, the *htz1Δ* mutant, which encodes H2A.Z, did not show the same grouping (Figure 4.8). Considering Arp6 deletion was shown to improve memory effects it is not unlikely that Arp6 might have an inhibitory function on the SWR1 complex.  It is also important to note that H2A.Z induction into histones is a regulatory mechanism of gene expression and a DNA repair mechanisms[78] outside of its memory effects and so the phenotypes we see in *htz1Δ* and *arp6Δ* could be a result of or influenced by many other processes that are impacted by H2A.Z incorporation into histones. Three different chromatin-remodeling proteins showing disruptions in memory does indicate that chromatin remodeling is an important aspect of the memory effect.

As described in the introduction, one of the functions of the chromatin remodeling in the cell is that it allows for RNAPII to take a poised position at the promoter, ready to be activated. What we observe in the mutants therefore also fits with what we observed in the biological assays (Figure 4.10). Atg13 expression is notably higher in the first hour of second starvation than it was in the first hour of initial starvation even after the Atg13 was cleared in replenishment (Figure 4.10B). This supports the notion that the memory effect in yeast is underpinned by chromatin remodeling which allows faster transcription of primed genes. Furthermore, the *srb8Δ* mutant showed improvement in T50 through longer initial starvation periods that was greater than those found in WT strains (figure 4.6). Srb8 is a part of the mediator complex for RNAPII and seems to function as a repressor of RNAPII activity[71]. Which also fits with the notion that this form of memory is expressed through rapid re-activation of transcription.

## 5.4 The autophagic response in metabolic mutants is diverse, but difficult properly parse

The purpose of this experiment was to find memory effects in the autophagic response. One obvious line of inquiry is the connection of the mutants discovered to the core processes of autophagy and nitrogen metabolism. The mutants discovered in this group had few common traits making it harder to draw conclusions from them. Gbp2 regulates autophagy by regulating the activity of the catalytic subdomains of PKA independently of the cAMP pathway. The *gbp2Δ* mutant shows an extreme reduction in T50 values (figure 4.6) with longer initial starvation indicating that it Gbp2 might mediate a response that down-regulates memory in some way. Ure2 controls the localization of the transcription factors Gln3 and Gat1[75] in response to TORC1 signaling. Gln3 and Gat1 activity leads to the expression of proteins that adapt the cell to inferior nitrogen sources. Notably, Ure2 has a prionic form, [URE3]. Prions have been theorized to be a potential memory mechanism. There is an increase in T50 and a decrease in autophagy max of *ure2Δ* which could indicate the disruption of a memory effect. Another of the mutants that showed a difference in parameters strongly outside the scope of WT strains was *sac1Δ*. The Sac1 lipid phosphatase dephosphorylates PtdIns4P molecules, altering the signaling on the surface of organelles including autophagosomes[74]. It could be that by modulating the lipid composition of autophagosomes Sac1 was a downstream effector of a memory effect, however it seems just as likely that the

long starvation periods were compromising the function of the protein and what appears to be an impaired memory effect is simply a cumulative effect of an impaired autophagy process. The reduced autophagy response in Ure2 could also be a consequence of an inability to properly adjust to the available nitrogen sources. Unfortunately, the problem with differentiating the effect of an impaired memory response from accumulating damage leading to impaired autophagy is hard to overcome and would likely require specifically designed experiments. There are other mutants that show a less exaggerated result, but still have a difference in T50 between 1 hour and 8hours around or below 0 in this screen, but they are harder to separate from the WT strains.

# Chapter 6

# Conclusions and next steps

## 6.1 Conclusions

In the aims we summarized this project into two fundamental questions. 1) Does *S. cerevisiae* display a memory effect when repeatedly exposed to nitrogen starvation and how long a starvation period is need before this effect becomes apparent in the response? And 2) Are there specific proteins that serve as a regulatory mechanism of this effect and if there are how does this regulation occur.

To answer the first question, we conducted an experiment growing *S. cerevisiae* through a cycle of nitrogen starvation, replenishment, and a second phase of nitrogen starvation with varying lengths of initial starvation and replenishment. The result from these experiments showed a clear effect on the second starvation based on the initial one, giving credence to the notion that the autophagy response in yeast has a memory component. We observed an improvement in the autophagy response of the second starvation happening when the cell had been in 5 hours or more of initial starvation. Notably, this effect persisted even when the replenishment period was prolonged.

Using information from the results of the first experiments we designed a genetic screen with 67 yeast mutants grown through 1, 4, and 8 hours of initial starvation, 4 hours of replenishment, and 12 hours of second starvation. From this screening we found mutants showing a memory response that was better than that of WT strains and some mutants performing notably worse than WT cells. Some of these mutants had direct links to established mechanisms of memory and others to nitrogen metabolism in yeast. To further clarify the mechanisms of the memory response in yeast we performed two sets of biological assays examining the phosphorylation of Atg13 and the expression levels of Atg13. With both showing an improvement in the autophagy response in the cell. Looking at the mutants, the two assays, and established research on memory effects it seems likely that at least part of the

memory response to autophagy takes the form of chromatin remodeling that drives the re-expression of Atg-related genes.

## 6.2 Next steps

This project is very much a starting point for research on the memory effect in yeast and it is my profound hope that the results gathered from these experiments will help to serve as building blocks to further elucidate the process. One potential next step is to take the mutants found in the screening and assay the expression of Atg13 or another autophagy related protein in them to see if they show a disruption in expression levels. Furthermore, many of the mutants examined show no difference in T50 between 1 hour and 8 hours of initial starvation, but because the results aren't extreme enough it is difficult to properly separate them from WT strains. By growing repeating the experiment with more replicates it might become possible to separate them further which could add to our understanding of the process. Furthermore, it is very likely that many components of the autophagic memory machinery were not covered by this screening and so expanding the screen seems like a viable path forward. Outside of further screening it might also be interesting to see if a heterokaryon experiment like the one executed to examine the GAL genes could be performed to see if autophagy has cytosolic components driving memory in the same way that the GAL genes do. This thesis is just a small introduction to a potentially much bigger field in autophagy and so the opportunities to expand on this work are plentiful.

# Bibliography


1. Galluzzi, L., et al., *Metabolic control of autophagy.* Cell, 2014. **159**(6): p. 1263-76. DOI: 10.1016/j.cell.2014.11.006.
2. Ohsumi, Y., *Historical landmarks of autophagy research.* Cell Research, 2014. **24**(1): p. 9-23. DOI: 10.1038/cr.2013.169.
3. Pfeifer, U. and M. Warmuth-Metz, *Inhibition by insulin of cellular autophagy in proximal tubular cells of rat kidney.* Am J Physiol, 1983. **244**(2): p. E109-14. DOI: 10.1152/ajpendo.1983.244.2.E109.
4. Mortimore, G.E., N.J. Hutson, and C.A. Surmacz, *Quantitative correlation between proteolysis and macro- and microautophagy in mouse hepatocytes during starvation and refeeding.* Proc Natl Acad Sci U S A, 1983. **80**(8): p. 2179-83. DOI: 10.1073/pnas.80.8.2179.
5. Tsukada, M. and Y. Ohsumi, *Isolation and characterization of autophagy-defective mutants of Saccharomyces cerevisiae.* FEBS Lett, 1993. **333**(1-2): p. 169-74. DOI: 10.1016/0014-5793(93)80398-e.
6. Parzych, K.R., et al., *A newly characterized vacuolar serine carboxypeptidase, Atg42/Ybr139w, is required for normal vacuole function and the terminal steps of autophagy in the yeast Saccharomyces cerevisiae.* Mol Biol Cell, 2018. **29**(9): p. 1089-1099. DOI: 10.1091/mbc.E17-08-0516.
7. Park, H., J.H. Kang, and S. Lee, *Autophagy in Neurodegenerative Diseases: A Hunter for Aggregates.* Int J Mol Sci, 2020. **21**(9). DOI: 10.3390/ijms21093369.
8. Namkoong, S., et al., *Autophagy Dysregulation and Obesity-Associated Pathologies.* Mol Cells, 2018. **41**(1): p. 3-10. DOI: 10.14348/molcells.2018.2213.
9. Bhattacharya, D., et al., *Is autophagy associated with diabetes mellitus and its complications? A review.* EXCLI J, 2018. **17**: p. 709-720. DOI: 10.17179/excli2018-1353.
10. Yun, C.W. and S.H. Lee, *The Roles of Autophagy in Cancer.* Int J Mol Sci, 2018. **19**(11). DOI: 10.3390/ijms19113466.
11. Li, W.W., J. Li, and J.K. Bao, *Microautophagy: lesser-known self-eating.* Cell Mol Life Sci, 2012. **69**(7): p. 1125-36. DOI: 10.1007/s00018-011-0865-5.
12. Sahu, R., et al., *Microautophagy of cytosolic proteins by late endosomes.* Dev Cell, 2011. **20**(1): p. 131-9. DOI: 10.1016/j.devcel.2010.12.003.
13. Kaushik, S. and A.M. Cuervo, *The coming of age of chaperone-mediated autophagy.* Nat Rev Mol Cell Biol, 2018. **19**(6): p. 365-381. DOI: 10.1038/s41580-018-0001-6.
14. Feng, Y., et al., *The machinery of macroautophagy.* Cell Res, 2014. **24**(1): p. 24-41. DOI: 10.1038/cr.2013.168.
15. Gaubitz, C., et al., *Molecular Basis of the Rapamycin Insensitivity of Target Of Rapamycin Complex 2.* Mol Cell, 2015. **58**(6): p. 977-88. DOI: 10.1016/j.molcel.2015.04.031.
16. Cybulski, N. and M.N. Hall, *TOR complex 2: a signaling pathway of its own.* Trends Biochem Sci, 2009. **34**(12): p. 620-7. DOI: 10.1016/j.tibs.2009.09.004.
17. Gonzalez, S. and C. Rallis, *The TOR Signaling Pathway in Spatial and Temporal Control of Cell Size and Growth.* Front Cell Dev Biol, 2017. **5**: p. 61. DOI: 10.3389/fcell.2017.00061.
18. Tatebe, H. and K. Shiozaki, *Evolutionary Conservation of the Components in the TOR Signaling Pathways.* Biomolecules, 2017. **7**(4). DOI: 10.3390/biom7040077.
19. Gonzalez, A. and M.N. Hall, *Nutrient sensing and TOR signaling in yeast and mammals.* EMBO J, 2017. **36**(4): p. 397-408. DOI: 10.15252/embj.201696010.

20. Binda, M., et al., *The Vam6 GEF controls TORC1 by activating the EGO complex.* Mol Cell, 2009. **35**(5): p. 563-73. DOI: 10.1016/j.molcel.2009.06.033.
21. Kim, D.H., et al., *GbetaL, a positive regulator of the rapamycin-sensitive pathway required for the nutrient-sensitive interaction between raptor and mTOR.* Mol Cell, 2003. **11**(4): p. 895-904. DOI: 10.1016/s1097-2765(03)00114-x.
22. Kira, S., et al., *Dynamic relocation of the TORC1-Gtr1/2-Ego1/2/3 complex is regulated by Gtr1 and Gtr2.* Mol Biol Cell, 2016. **27**(2): p. 382-96. DOI: 10.1091/mbc.E15-07-0470.
23. Betz, C. and M.N. Hall, *Where is mTOR and what is it doing there?* J Cell Biol, 2013. **203**(4): p. 563-74. DOI: 10.1083/jcb.201306041.
24. Kira, S., et al., *Reciprocal conversion of Gtr1 and Gtr2 nucleotide-binding states by Npr2-Npr3 inactivates TORC1 and induces autophagy.* Autophagy, 2014. **10**(9): p. 1565-78. DOI: 10.4161/auto.29397.
25. Sancak, Y., et al., *The Rag GTPases bind raptor and mediate amino acid signaling to mTORC1.* Science, 2008. **320**(5882): p. 1496-501. DOI: 10.1126/science.1157535.
26. Stephan, J.S., et al., *The Tor and PKA signaling pathways independently target the Atg1/Atg13 protein kinase complex to control autophagy.* Proc Natl Acad Sci U S A, 2009. **106**(40): p. 17049-54. DOI: 10.1073/pnas.0903316106.
27. Budovskaya, Y.V., et al., *The Ras/cAMP-dependent protein kinase signaling pathway regulates an early step of the autophagy process in Saccharomyces cerevisiae.* J Biol Chem, 2004. **279**(20): p. 20663-71. DOI: 10.1074/jbc.M400272200.
28. Yang, Z. and D.J. Klionsky, *An overview of the molecular mechanism of autophagy.* Curr Top Microbiol Immunol, 2009. **335**: p. 1-32. DOI: 10.1007/978-3-642-00302-8_1.
29. Kabeya, Y., et al., *Characterization of the Atg17-Atg29-Atg31 complex specifically required for starvation-induced autophagy in Saccharomyces cerevisiae.* Biochem Biophys Res Commun, 2009. **389**(4): p. 612-5. DOI: 10.1016/j.bbrc.2009.09.034.
30. Cheong, H., et al., *The Atg1 kinase complex is involved in the regulation of protein recruitment to initiate sequestering vesicle formation for nonspecific autophagy in Saccharomyces cerevisiae.* Mol Biol Cell, 2008. **19**(2): p. 668-81. DOI: 10.1091/mbc.e07-08-0826.
31. Legakis, J.E., W.L. Yen, and D.J. Klionsky, *A cycling protein complex required for selective autophagy.* Autophagy, 2007. **3**(5): p. 422-32. DOI: 10.4161/auto.4129.
32. Yamamoto, H., et al., *Atg9 vesicles are an important membrane source during early steps of autophagosome formation.* J Cell Biol, 2012. **198**(2): p. 219-33. DOI: 10.1083/jcb.201202061.
33. Sawa-Makarska, J., et al., *Reconstitution of autophagosome nucleation defines Atg9 vesicles as seeds for membrane formation.* Science, 2020. **369**(6508). DOI: 10.1126/science.aaz7714.
34. Karanasios, E., et al., *Autophagy initiation by ULK complex assembly on ER tubulovesicular regions marked by ATG9 vesicles.* Nat Commun, 2016. **7**: p. 12420. DOI: 10.1038/ncomms12420.
35. Hanada, T., et al., *The Atg12-Atg5 conjugate has a novel E3-like activity for protein lipidation in autophagy.* J Biol Chem, 2007. **282**(52): p. 37298-302. DOI: 10.1074/jbc.C700195200.
36. Abdollahzadeh, I., et al., *The Atg8 Family of Proteins-Modulating Shape and Functionality of Autophagic Membranes.* Front Genet, 2017. **8**: p. 109. DOI: 10.3389/fgene.2017.00109.
37. Yu, L., Y. Chen, and S.A. Tooze, *Autophagy pathway: Cellular and molecular mechanisms.* Autophagy, 2018. **14**(2): p. 207-215. DOI: 10.1080/15548627.2017.1378838.
38. Conrad, M., et al., *Nutrient sensing and signaling in the yeast Saccharomyces cerevisiae.* FEMS Microbiol Rev, 2014. **38**(2): p. 254-99. DOI: 10.1111/1574-6976.12065.
39. Bonfils, G., et al., *Leucyl-tRNA synthetase controls TORC1 via the EGO complex.* Mol Cell, 2012. **46**(1): p. 105-10. DOI: 10.1016/j.molcel.2012.02.009.
40. Berry, D.B. and A.P. Gasch, *Stress-activated genomic expression changes serve a preparative role for impending stress in yeast.* Mol Biol Cell, 2008. **19**(11): p. 4580-7. DOI: 10.1091/mbc.E07-07-0680.

41. Tafur, L., et al., *Cryo-EM structure of the SEA complex.* Nature, 2022. **611**(7935): p. 399-404. DOI: 10.1038/s41586-022-05370-0.
42. Lee, J.H., U.S. Cho, and M. Karin, *Sestrin regulation of TORC1: Is Sestrin a leucine sensor?* Sci Signal, 2016. **9**(431): p. re5. DOI: 10.1126/scisignal.aaf2885.
43. Chantranupong, L., et al., *The CASTOR Proteins Are Arginine Sensors for the mTORC1 Pathway.* Cell, 2016. **165**(1): p. 153-164. DOI: 10.1016/j.cell.2016.02.035.
44. Tanigawa, M. and T. Maeda, *An In Vitro TORC1 Kinase Assay That Recapitulates the Gtr-Independent Glutamine-Responsive TORC1 Activation Mechanism on Yeast Vacuoles.* Mol Cell Biol, 2017. **37**(14). DOI: 10.1128/MCB.00075-17.
45. Tanigawa, M., et al., *A glutamine sensor that directly activates TORC1.* Commun Biol, 2021. **4**(1): p. 1093. DOI: 10.1038/s42003-021-02625-w.
46. D'Urso, A. and J.H. Brickner, *Epigenetic transcriptional memory.* Curr Genet, 2017. **63**(3): p. 435-439. DOI: 10.1007/s00294-016-0661-8.
47. Stockwell, S.R., C.R. Landry, and S.A. Rifkin, *The yeast galactose network as a quantitative model for cellular memory.* Mol Biosyst, 2015. **11**(1): p. 28-37. DOI: 10.1039/c4mb00448e.
48. O'Kane, C.J. and E.M. Hyland, *Yeast epigenetics: the inheritance of histone modification states.* Biosci Rep, 2019. **39**(5). DOI: 10.1042/BSR20182006.
49. D'Urso, A. and J.H. Brickner, *Mechanisms of epigenetic memory.* Trends Genet, 2014. **30**(6): p. 230-6. DOI: 10.1016/j.tig.2014.04.004.
50. Brickner, J.H., *Transcriptional memory at the nuclear periphery.* Curr Opin Cell Biol, 2009. **21**(1): p. 127-33. DOI: 10.1016/j.ceb.2009.01.007.
51. Light, W.H., et al., *Interaction of a DNA zip code with the nuclear pore complex promotes H2A.Z incorporation and INO1 transcriptional memory.* Mol Cell, 2010. **40**(1): p. 112-25. DOI: 10.1016/j.molcel.2010.09.007.
52. Tan-Wong, S.M., H.D. Wijayatilake, and N.J. Proudfoot, *Gene loops function to maintain transcriptional memory through interaction with the nuclear pore complex.* Genes Dev, 2009. **23**(22): p. 2610-24. DOI: 10.1101/gad.1823209.
53. D'Urso, A., et al., *Set1/COMPASS and Mediator are repurposed to promote epigenetic transcriptional memory.* Elife, 2016. **5**. DOI: 10.7554/eLife.16691.
54. Hyun, K., et al., *Writing, erasing and reading histone lysine methylations.* Exp Mol Med, 2017. **49**(4): p. e324. DOI: 10.1038/emm.2017.11.
55. Marques, M., et al., *Reconciling the positive and negative roles of histone H2A.Z in gene transcription.* Epigenetics, 2010. **5**(4): p. 267-72. DOI: 10.4161/epi.5.4.11520.
56. Brickner, D.G., et al., *H2A.Z-mediated localization of genes at the nuclear periphery confers epigenetic memory of previous transcriptional state.* PLoS Biol, 2007. **5**(4): p. e81. DOI: 10.1371/journal.pbio.0050081.
57. Fan, J., et al., *H2A.Z deposition by SWR1C involves multiple ATP-dependent steps.* Nat Commun, 2022. **13**(1): p. 7052. DOI: 10.1038/s41467-022-34861-x.
58. Kundu, S., P.J. Horn, and C.L. Peterson, *SWI/SNF is required for transcriptional memory at the yeast GAL gene cluster.* Genes Dev, 2007. **21**(8): p. 997-1004. DOI: 10.1101/gad.1506607.
59. Zacharioudakis, I., T. Gligoris, and D. Tzamarias, *A yeast catabolic enzyme controls transcriptional memory.* Curr Biol, 2007. **17**(23): p. 2041-6. DOI: 10.1016/j.cub.2007.10.044.
60. Chernova, T.A., Y.O. Chernoff, and K.D. Wilkinson, *Prion-based memory of heat stress in yeast.* Prion, 2017. **11**(3): p. 151-161. DOI: 10.1080/19336896.2017.1328342.
61. Liebman, S.W. and Y.O. Chernoff, *Prions in yeast.* Genetics, 2012. **191**(4): p. 1041-72. DOI: 10.1534/genetics.111.137760.
62. Shorter, J. and S. Lindquist, *Hsp104 catalyzes formation and elimination of self-replicating Sup35 prion conformers.* Science, 2004. **304**(5678): p. 1793-7. DOI: 10.1126/science.1098007.
63. Chakrabortee, S., et al., *Intrinsically Disordered Proteins Drive Emergence and Inheritance of Biological Traits.* Cell, 2016. **167**(2): p. 369-381 e12. DOI: 10.1016/j.cell.2016.09.017.

64. Duina, A.A., M.E. Miller, and J.B. Keeney, *Budding yeast for budding geneticists: a primer on the Saccharomyces cerevisiae model system.* Genetics, 2014. **197**(1): p. 33-48. DOI: 10.1534/genetics.114.163188.
65. Yu, R. and J. Nielsen, *Yeast systems biology in understanding principles of physiology underlying complex human diseases.* Curr Opin Biotechnol, 2020. **63**: p. 63-69. DOI: 10.1016/j.copbio.2019.11.021.
66. Giaever, G., et al., *Functional profiling of the Saccharomyces cerevisiae genome.* Nature, 2002. **418**(6896): p. 387-91. DOI: 10.1038/nature00935.
67. Brachmann, C.B., et al., *Designer deletion strains derived from Saccharomyces cerevisiae S288C: a useful set of strains and plasmids for PCR-mediated gene disruption and other applications.* Yeast, 1998. **14**(2): p. 115-32. DOI: 10.1002/(SICI)1097-0061(19980130)14:2<115::AID-YEA204>3.0.CO;2-2.
68. Urban, J., et al., *Sch9 is a major target of TORC1 in Saccharomyces cerevisiae.* Mol Cell, 2007. **26**(5): p. 663-74. DOI: 10.1016/j.molcel.2007.04.020.
69. Wu, W.H., et al., *Swc2 is a widely conserved H2AZ-binding module essential for ATP-dependent histone exchange.* Nat Struct Mol Biol, 2005. **12**(12): p. 1064-71. DOI: 10.1038/nsmb1023.
70. Workman, J.J., H. Chen, and R.N. Laribee, *Saccharomyces cerevisiae TORC1 Controls Histone Acetylation by Signaling Through the Sit4/PP6 Phosphatase to Regulate Sirtuin Deacetylase Nuclear Accumulation.* Genetics, 2016. **203**(4): p. 1733-46. DOI: 10.1534/genetics.116.188458.
71. Ansari, S.A. and R.H. Morse, *Mechanisms of Mediator complex action in transcriptional activation.* Cell Mol Life Sci, 2013. **70**(15): p. 2743-56. DOI: 10.1007/s00018-013-1265-9.
72. Lu, A. and J.P. Hirsch, *Cyclic AMP-independent regulation of protein kinase A substrate phosphorylation by Kelch repeat proteins.* Eukaryot Cell, 2005. **4**(11): p. 1794-800. DOI: 10.1128/EC.4.11.1794-1800.2005.
73. Muramoto, M., et al., *Essential roles of phosphatidylinositol 4-phosphate phosphatases Sac1p and Sjl3p in yeast autophagosome formation.* Biochim Biophys Acta Mol Cell Biol Lipids, 2022. **1867**(9): p. 159184. DOI: 10.1016/j.bbalip.2022.159184.
74. Zhang, H., et al., *PtdIns4P restriction by hydrolase SAC1 decides specific fusion of autophagosomes with lysosomes.* Autophagy, 2021. **17**(8): p. 1907-1917. DOI: 10.1080/15548627.2020.1796321.
75. Cooper, T.G., *Transmitting the signal of excess nitrogen in Saccharomyces cerevisiae from the Tor proteins to the GATA factors: connecting the dots.* FEMS Microbiol Rev, 2002. **26**(3): p. 223-38. DOI: 10.1111/j.1574-6976.2002.tb00612.x.
76. Chen, L.J., E.B. Sawyer, and S. Perrett, *The yeast prion protein Ure2: insights into the mechanism of amyloid formation.* Biochem Soc Trans, 2011. **39**(5): p. 1359-64. DOI: 10.1042/BST0391359.
77. Gonzalez, A., et al., *TORC1 promotes phosphorylation of ribosomal protein S6 via the AGC kinase Ypk3 in Saccharomyces cerevisiae.* PLoS One, 2015. **10**(3): p. e0120250. DOI: 10.1371/journal.pone.0120250.
78. Larschan, E. and F. Winston, *The Saccharomyces cerevisiae Srb8-Srb11 complex functions with the SAGA complex during Gal4-activated transcription.* Mol Cell Biol, 2005. **25**(1): p. 114-23. DOI: 10.1128/MCB.25.1.114-123.2005.

# Chapter 7

# Appendix – Supplementary figures

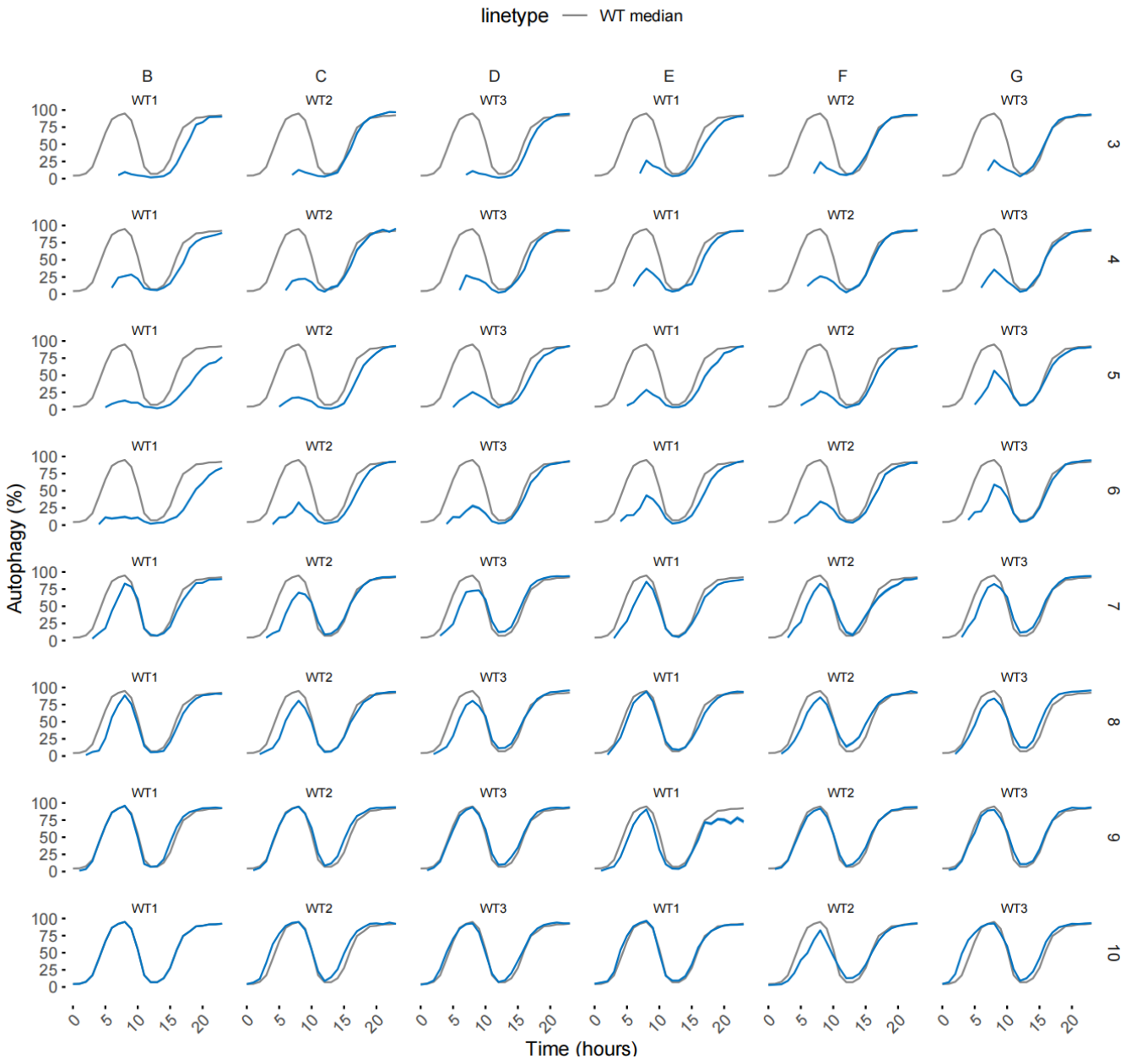


**Figure S1: Raw predictions from the first study of the autophagic response in memory.** The raw autophagy predictions from cells with initial starvation times between 1-8 hours and a replenishment of 4 hours. The grey line represents a WT1 strain grown through 8 hours of initial starvation.

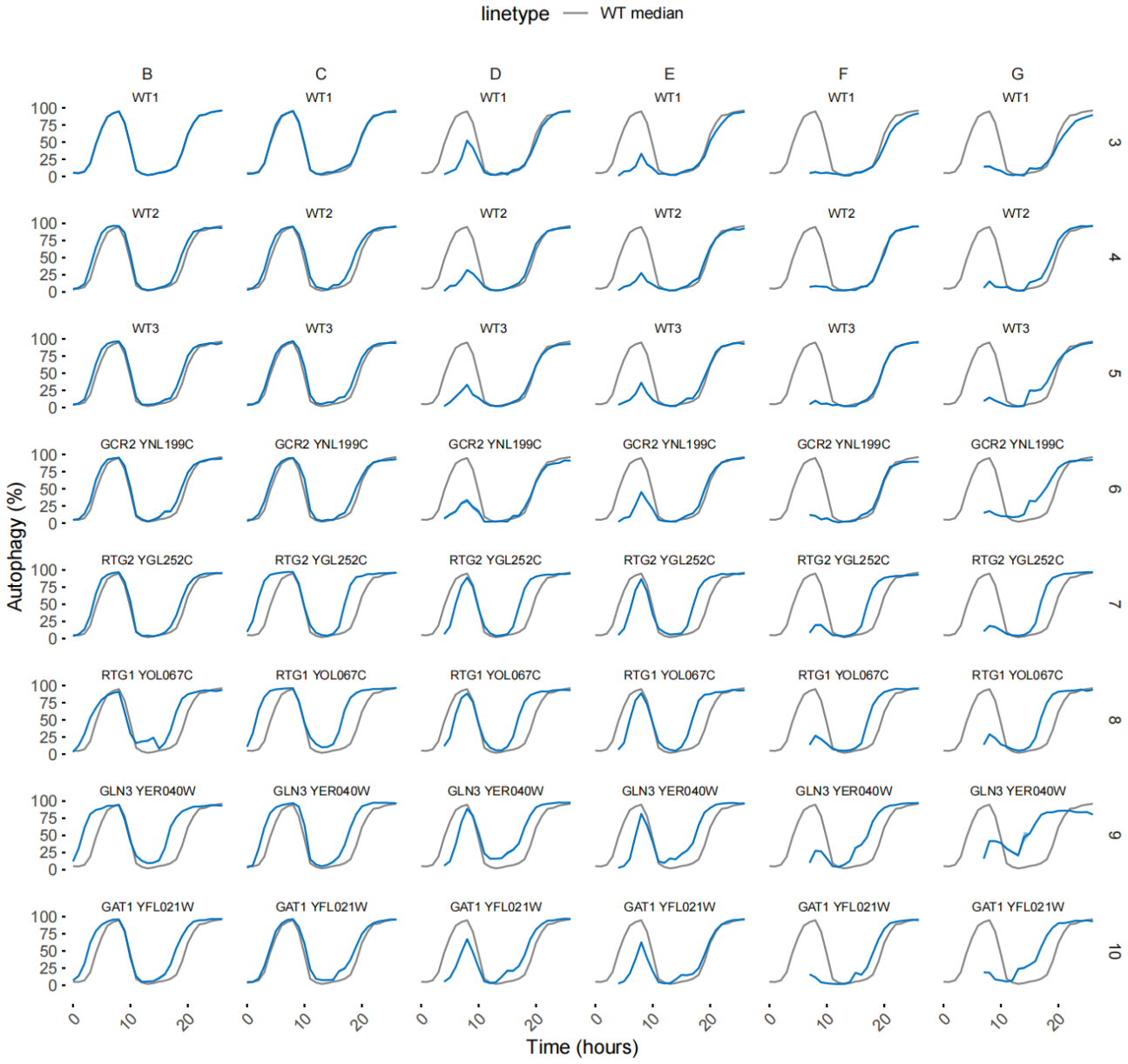


**Figure S2: Raw predictions from the second study of the autophagic response in memory.** The raw autophagy predictions from cells with initial starvation times of 1 hour, 4 hours or 8 hours and a replenishment of 7 hours. The grey line represents a WT1 strain grown through 8 hours of initial starvation. This line of experiments also used several TFs that were not used in the final thesis. One out of two replicates shown.

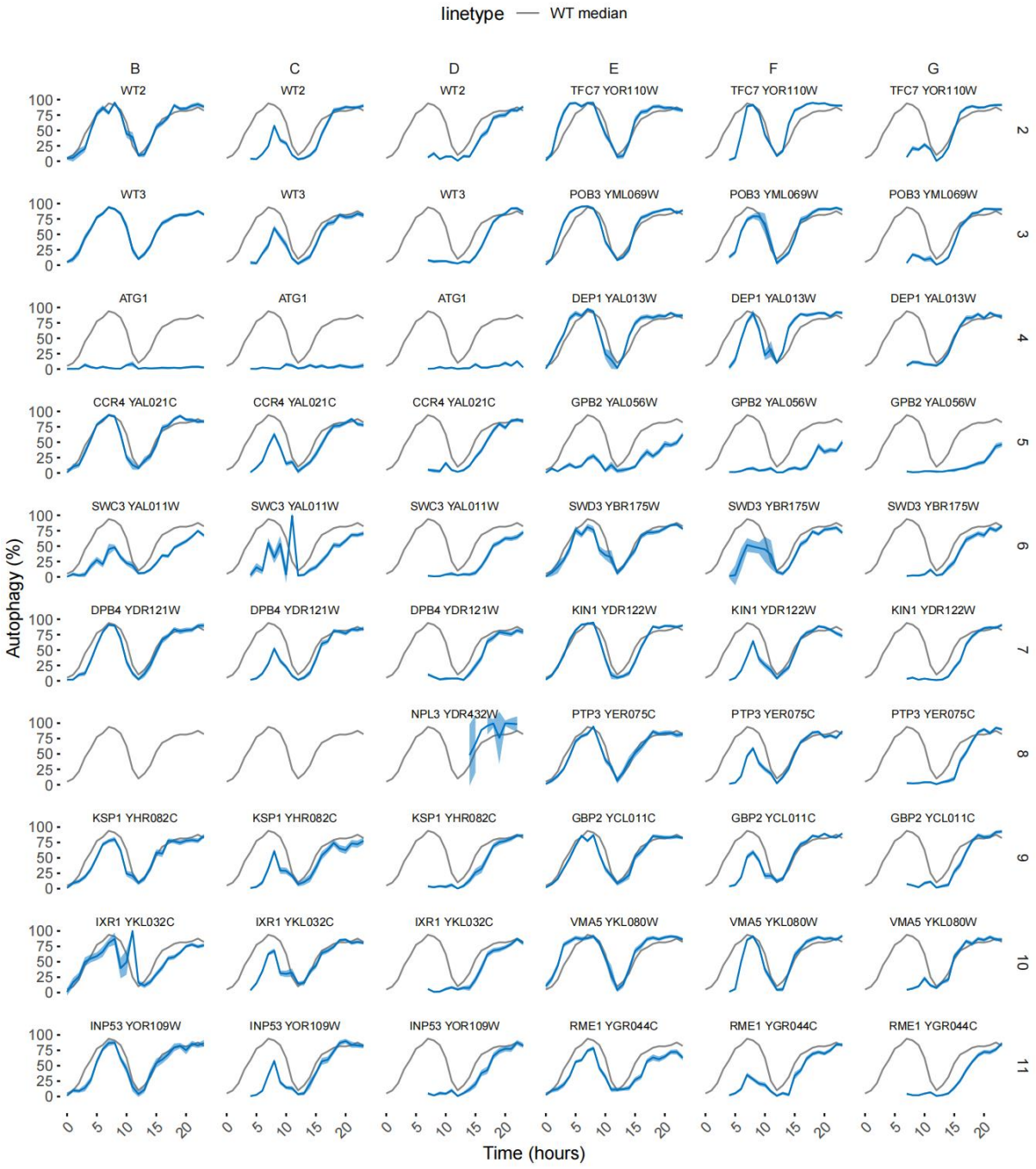


**Figure S3: Raw predictions from the first plate in the large scale screen.** The raw autophagy predictions from mutants with initial starvation times of 1 hour, 4 hours or 8 hours and a replenishment of 4 hours. The grey line represents a WT3 strain grown through 8 hours of initial starvation.

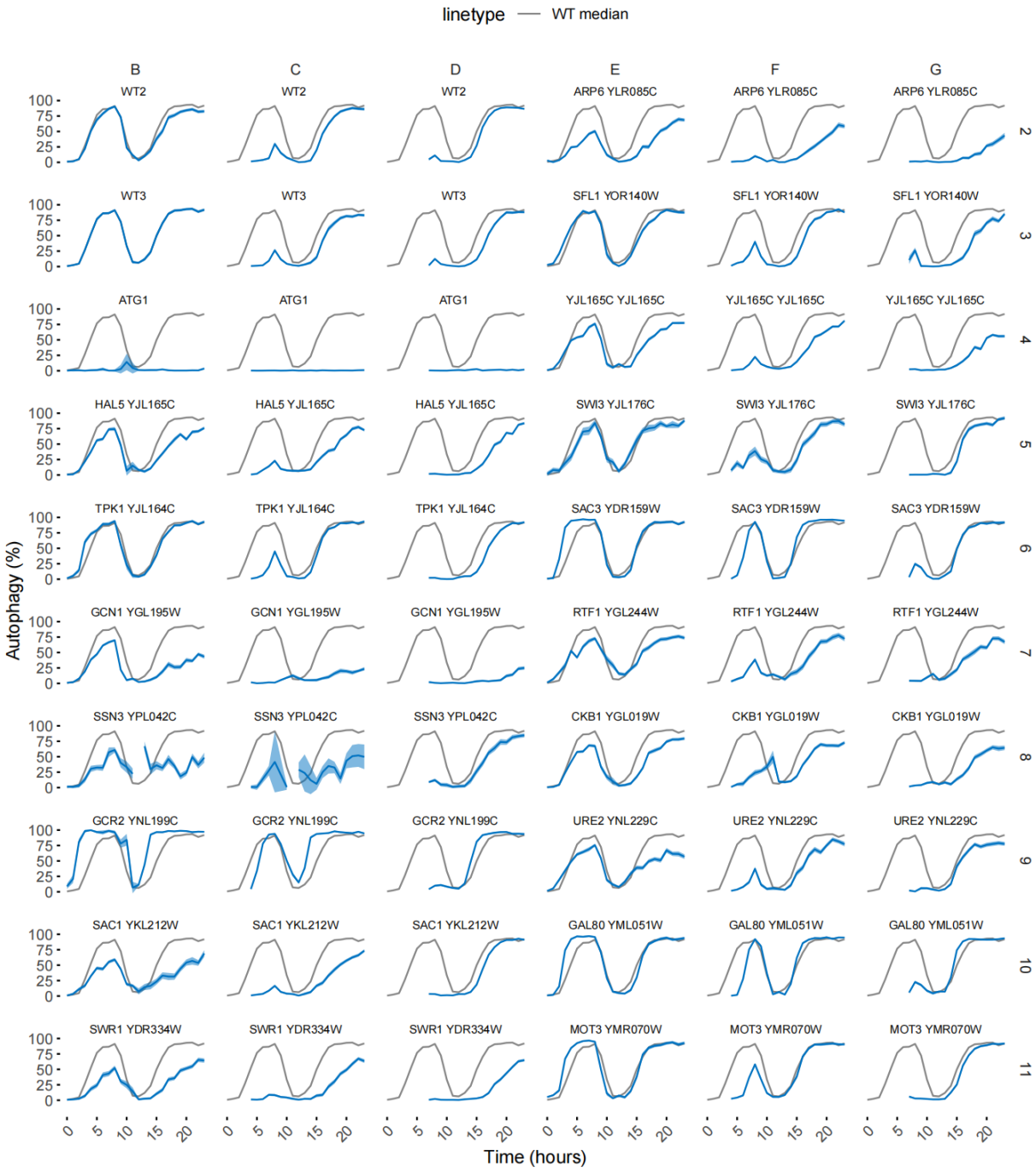


**Figure S4: Raw predictions from the second plate in the large scale screen.** The raw autophagy predictions from mutants with initial starvation times of 1 hour, 4 hours or 8 hours and a replenishment of 4 hours. The grey line represents a WT3 strain grown through 8 hours of initial starvation.

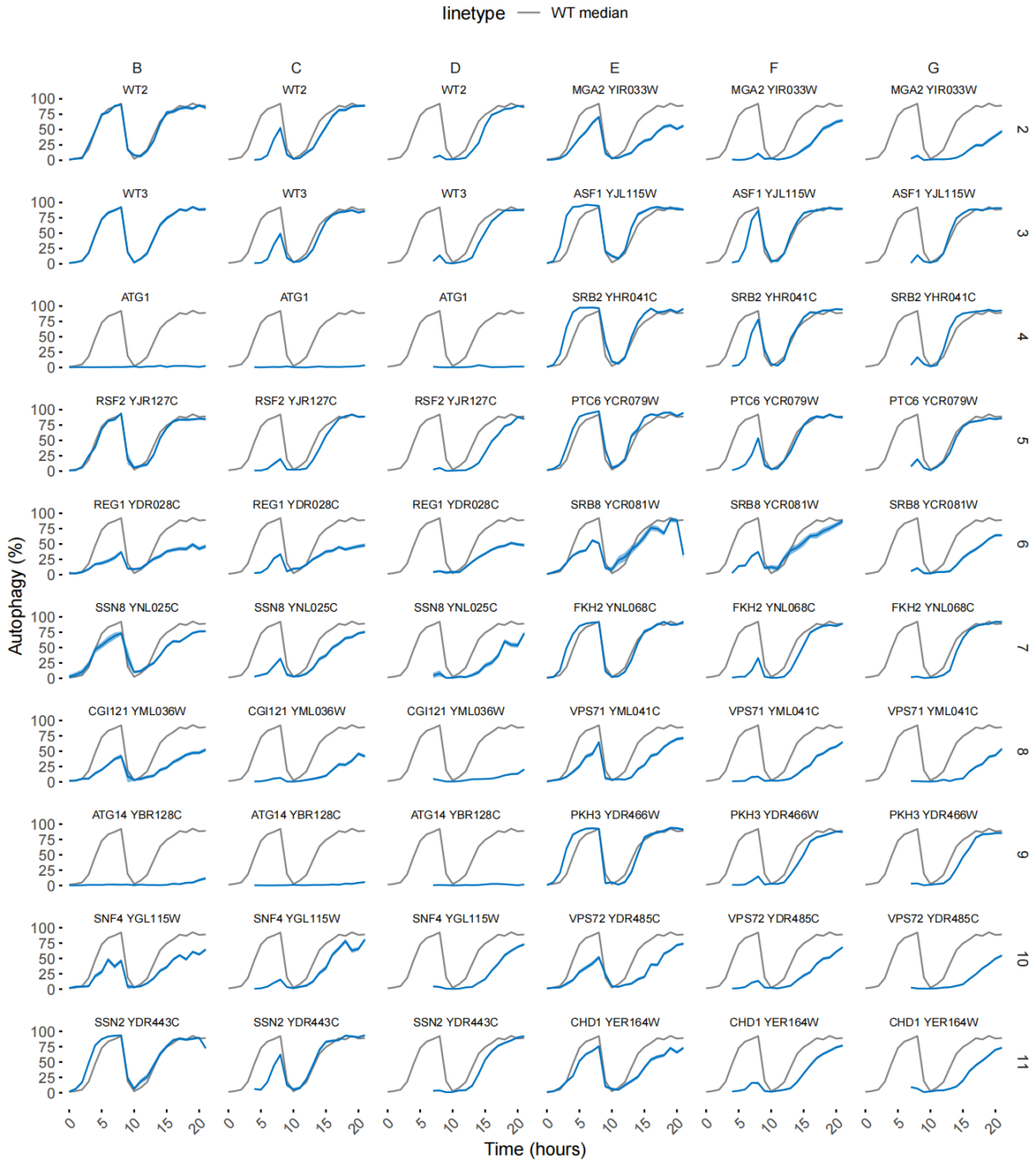


**Figure S5: Raw predictions from the third plate in the large scale screen.** The raw autophagy predictions from mutants with initial starvation times of 1 hour, 4 hours or 8 hours and a replenishment of 4 hours. The grey line represents a WT3 strain grown through 8 hours of initial starvation.

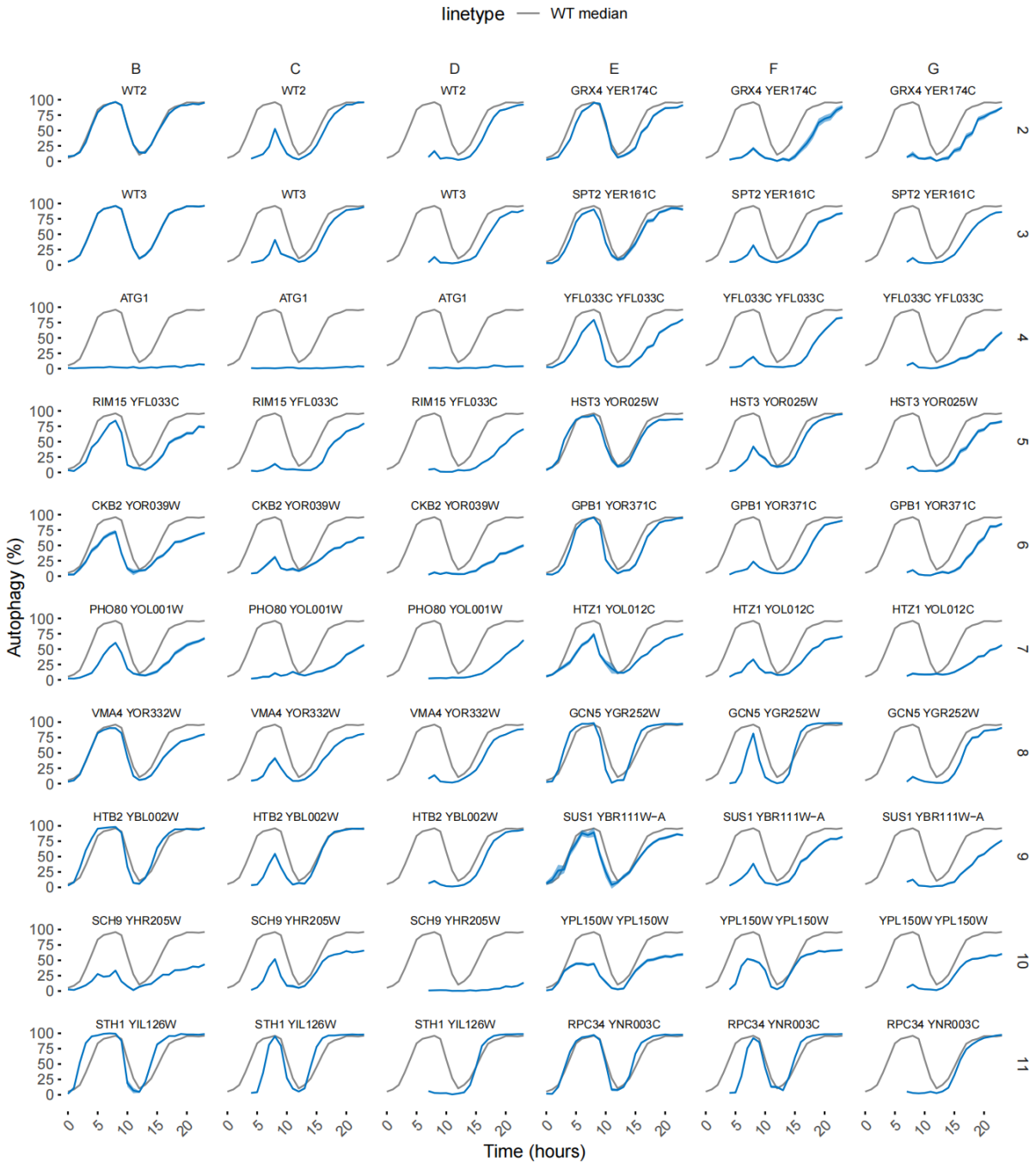


**Figure S6: Raw predictions from the fourth plate in the large scale screen.** The raw autophagy predictions from mutants with initial starvation times of 1 hour, 4 hours or 8 hours and a replenishment of 4 hours. The grey line represents a WT3 strain grown through 8 hours of initial starvation.

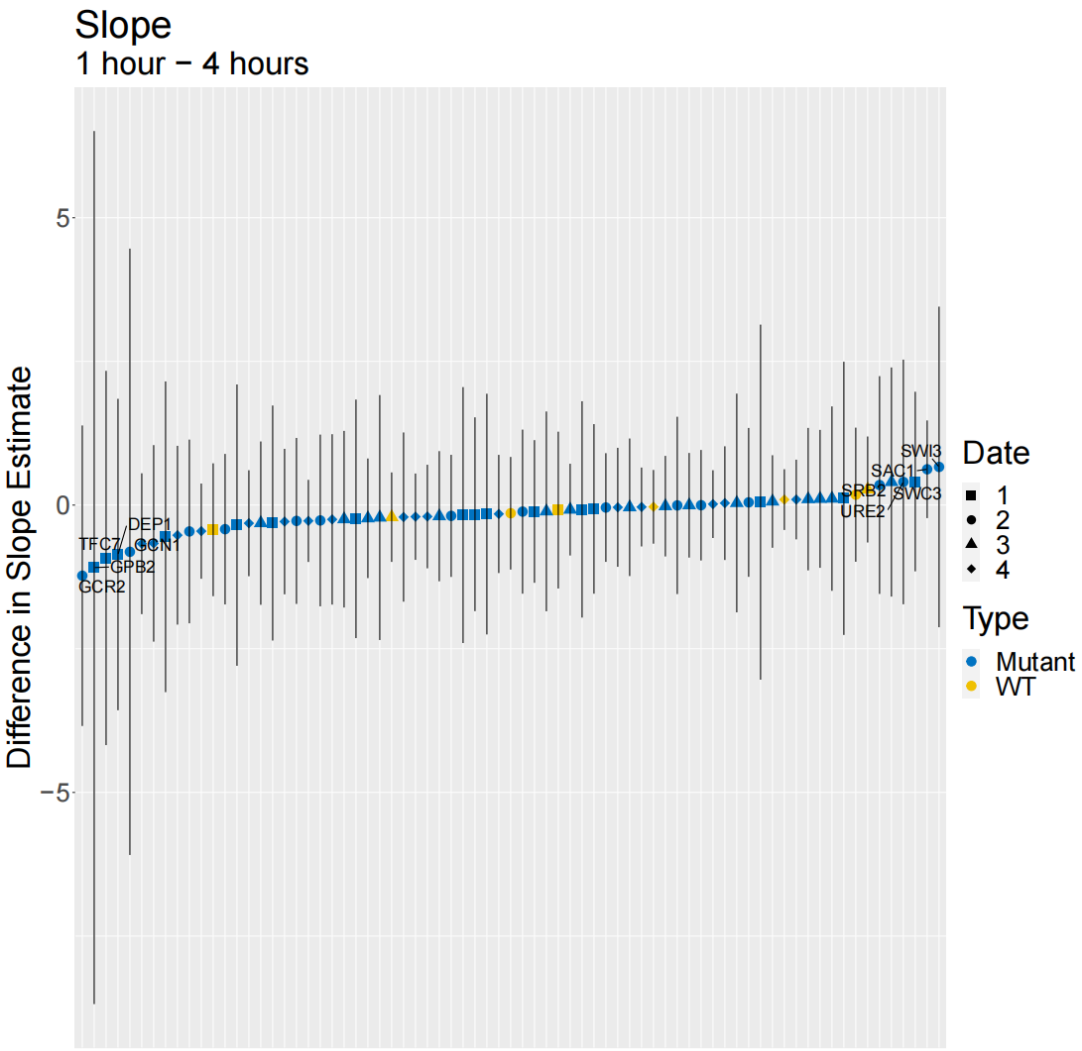


**Figure S7: Waterfall plot of the differences in slope parameter between 1 hour and 4 hours.** A plot showing the differences in the slope parameter in the mutant screen arranged in ascending order. Bars represent the error found in the parameter.

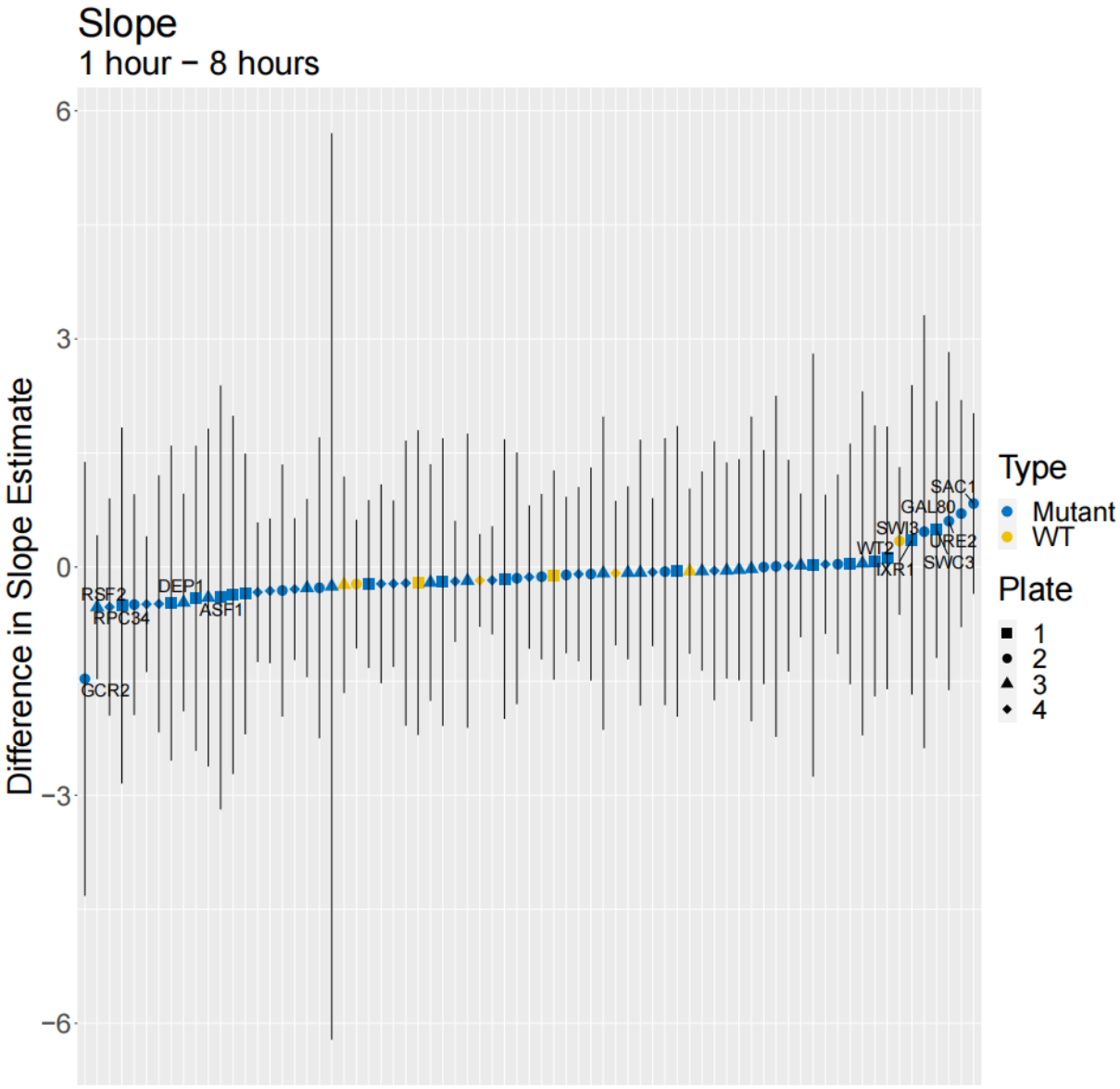


**Figure S8: Waterfall plot of the differences in slope parameter between 1 hour and 8 hours.** A plot showing the differences in the slope parameter in the mutant screen arranged in ascending order. Bars represent the error found in the parameter.

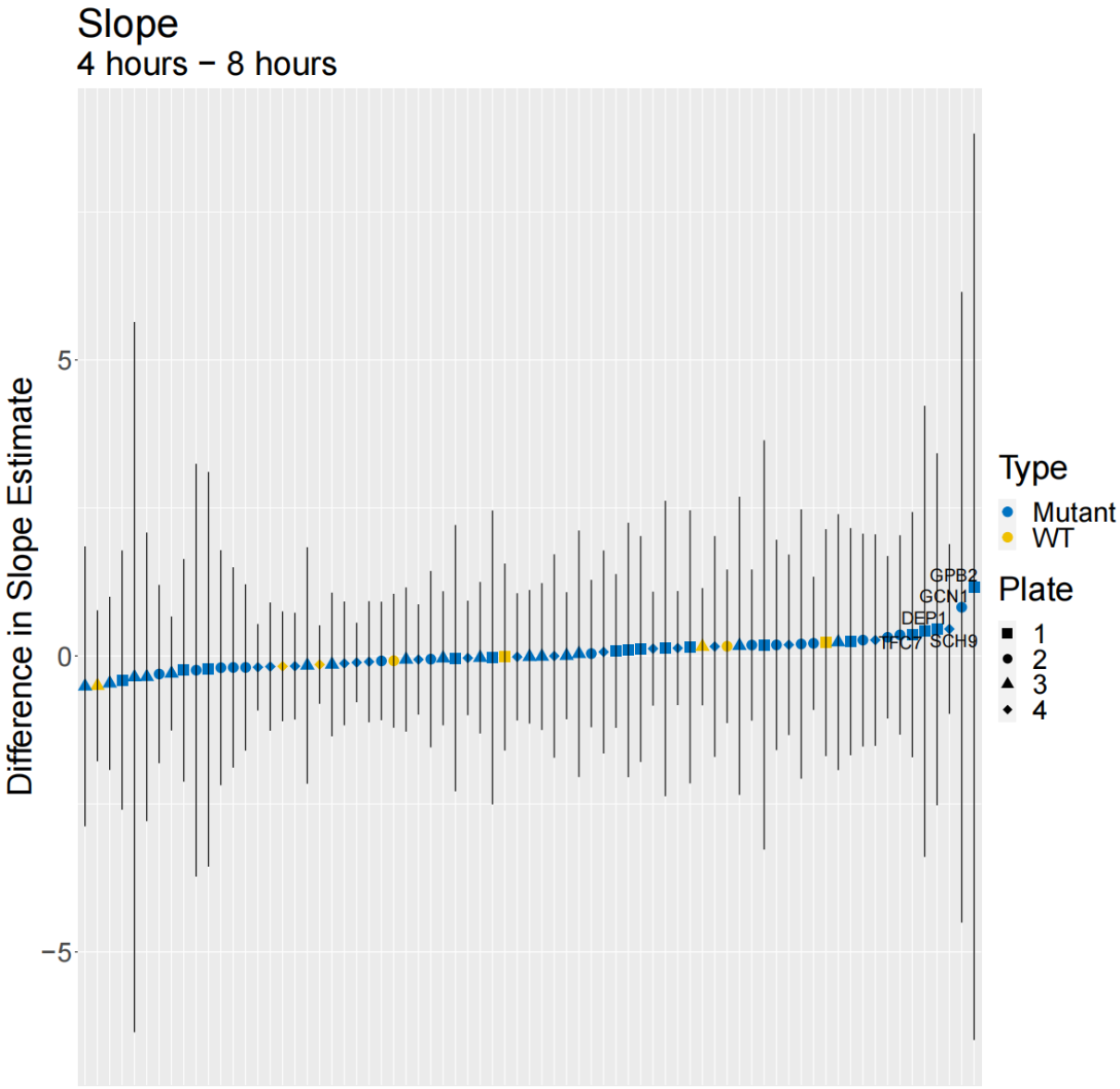


**Figure S9: Waterfall plot of the differences in slope parameter between 4 hours and 8 hours.** A plot showing the differences in the slope parameter in the mutant screen arranged in ascending order. Bars represent the error found in the parameter.